RESEARCH IN THE COAS
& OCEANIC ENVIRONMENT

Technical Report No. 2

An Experimental Study of Wind Velocity Profiles over a Wavy Surface

by

Francis J. Merceret

ONR N00014-69-A0407

COLLEGE OF MARINE STUDIES
UNIVERSITY OF DELAWARE
Newark, Delaware

125

AN EXPERIMENTAL STUDY

OF WIND VELOCITY PROFILES

OVER A WAVY SURFACE

by

Francis J. Merceret

Lecturer, College of Marine Studies
University of Delaware
Newark, Delaware 19711

Details of illustrations in
this document may be better
studied on microfiche

The text of this document is also submitted to the Department of Earth and Planetary Sciences, The Johns Hopkins University, Baltimore, Maryland, as a dissertation (1972, unpublished) for the degree of Doctor of Philosophy.

Supported by ONR Contract Number N00014-69-A-0407
Research in the Coastal and Oceanic Environment

Publication 2MS065 of the
College of Marine Studies
at the University of Delaware

Newark, Delaware 19711
April 1972

Unclassified
Security Classification

DOCUMENT CONTROL DATA - R & D

(Security classification of title, body of abstract and indexing annotation must be entered when the overall report is classified)

1. ORIGINATING ACTIVITY (Corporate author) University of Delaware	2a. REPORT SECURITY CLASSIFICATION Unclassified
	2b. GROUP

3. REPORT TITLE

An Experimental Study of Wind Velocity Profiles Over a Wavy Surface

4. DESCRIPTIVE NOTES (Type of report and inclusive dates)

Technical Report

5. AUTHOR(S) (First name, middle initial, last name)

Francis J. Merceret

6. REPORT DATE April, 1972	7a. TOTAL NO. OF PAGES 113	7b. NO. OF REFS 29
8a. CONTRACT OR GRANT NO. N00014-69-A-0407	9a. ORIGINATOR'S REPORT NUMBER(S) Technical Report No. 2	
b. PROJECT NO.		
c.	9b. OTHER REPORT NO(S) (Any other numbers that may be assigned this report) CMS No. 2MS065	
d.		

10. DISTRIBUTION STATEMENT

Distribution of this document is unlimited.

11. SUPPLEMENTARY NOTES	12. SPONSORING MILITARY ACTIVITY Geography Branch, Office of Naval Research, Arlington, Virginia 22217

13. ABSTRACT

Wind velocity profiles and turbulence measurements have been obtained over a plow corrugated field using hot-film and cup anemometers at sampling heights covering from 3 cm to 4 m. The profiles, based on averaging times from 5 to 15 minutes, fit the logarithmic model with correlation coefficients greater than 0.9 and with many greater than 0.97. The data support the conjecture of Ruggles (1970) that large and sporadic fluctuations in the roughness length and friction velocity observed over water are due to the generation of wind waves on the surface. Additional information regarding the response of the profile parameters to rapidly changing conditions is inferred from studies of profiles inside and outside of intermittent bursts of turbulent activity. The results indicate that mechanisms which involve steady state logarithmic mean velocity profiles in the wind above a water surface are not suitable to explain the generation of waves, since the data show the profile parameters to be markedly affected by the generation process.

DD FORM 1 NOV 65 1473 (PAGE 1)

S/N 0101-807-6801

Unclassified
Security Classification

Unclassified
Security Classification

14 KEY WORDS	LINK A		LINK B		LINK C	
	ROLE	WT	ROLE	WT	ROLE	WT
Waves						
Turbulence						
Wind profiles						
Air-sea interaction						

Unclassified
Security Classification

ABSTRACT

Wind velocity profiles and turbulence measurements have been obtained over a plow corrugated field using hot-film and cup anemometers at sampling heights covering from 3 cm to 4 m. The profiles, based on averaging times from 5 to 15 minutes, fit the logarithmic model with correlation coefficients greater than 0.9 and with many greater than 0.97. The data support the conjecture of Ruggles (1970) that large and sporadic fluctuations in the roughness length and friction velocity observed over water are due to the generation of wind waves on the surface. Additional information regarding the response of the profile parameters to rapidly changing conditions is inferred from studies of profiles inside and outside of intermittent bursts of turbulent activity. The results indicate that mechanisms which involve steady state logarithmic mean velocity profiles in the wind above a water surface are not suitable to explain the generation of waves, since the data show the profile parameters to be markedly affected by the generation process.

ACKNOWLEDGEMENTS

I have been fortunate to be able to work closely with several departments in two universities involved in research in atmospheric and oceanic physics. At The Johns Hopkins University I have had the benefit of consultation with Professor Owen Phillips, Earth and Planetary Sciences, during the entire project. During the calibration of the instruments I enjoyed the advice and support of Professor S. Corrsin, Mechanics, and the able assistance of Mr. Bernard Bertling, Mechanics. At The University of Delaware the Administration of the College of Marine Studies, especially Dean William S. Gaither, Mr. Lloyd Stiffler, and Mr. B.W. Howk, quickly obtained funds for the initiation of the research and provided continuing support as long as was possible. Ms. Mary Conner repeatedly harassed tardy suppliers to ensure that our equipment all arrived before the weather conditions deteriorated. In addition I was blessed with the indispensable support of an experienced atmospheric field research scientist, Mr. Richard T. Field of the Department of Geography, who loaned me not only his wind profile system but his time, his labor, and his knowledge.

A special consideration is due Dr. Blair Kinsman, under whom I've studied and worked at The Johns Hopkins and with whom I worked closely at Delaware. It was my good fortune to come to Delaware when he did. He provided a continuity of

contact and unification of diverse elements which contributed as much as anything else involved in the project to keeping it going on target scientifically and financially, and on time.

Persons outside the academic community also helped provide important support for the project. Ms. Hoagland Gates of Elkton, Maryland was kind enough to allow us to use her field and Mr. Mack Baily to let us use his airport. Mr. R.L. Humphrey and Mr. R. Suhoke of DISA S & B expended more than the usual effort to ensure we had functioning anemometers in the short time we had to work. My wife Elizabeth gave more than the customary moral support for the project. She helped survey the field site, take data, and process the data on the calculator.

A document like this requires skilled production support. Parts of the first draft were typed by Ms. Terese Detwiler, Ms. Linda Hibberd, and Ms. Diane Iffland of The College of Marine Studies of The University of Delaware. The semi-final draft was prepared by Ms. Hibberd who travelled through some rough winter weather to meet the deadlines I asked of her. The final copy was prepared by Ms. M. Kathy Shinn of Annapolis, Maryland, while the figures were produced at The Chesapeake Bay Institute of The Johns Hopkins University by Mr. William L. Wilson. All of these who helped create the

final work have my gratitude.

I am grateful as well to DISA S & B, General Radio, Heath Company, Lockheed Electronics, and C.W. Thornthwaite Associates for allowing me to reproduce their manufacturer's specifications.

Finally, the project was supported by the Office of Naval Research under Contract Number N00014-69-A0407, and by the National Science Foundation Under Grant Number GA-16603.

TABLE OF CONTENTS

LIST OF TABLES

LIST OF FIGURES

I. INTRODUCTION

The experiment described in this paper was conducted over land, yet it is directed towards understanding the generation of surface water waves by the turbulent wind. Because it is not immediately obvious that one ought investigate wave generation in a place where no waves are being generated, it seems appropriate to explain why and how the decision to make this particular investigation evolved.

In a series of papers, Miles (1957, 1959, 1960, 1962) presented a model which has become the basis for much of current research into the generation of surface waves by the wind. Expositions on and interpretations of the Miles model may be found in Lighthill (1962), Kinsman (1965), and Phillips (1966) among others, while a summary of the model and a discussion of its place in over-all wind wave theory is given in Shemdin and Hsu (1966). Because others have written so extensively on the subject, I will describe here only those features of the theory pertaining to the purposes and results of this investigation.

Miles calculated the energy and momentum transfer from a laminar shear flow of prescribed velocity profile to a train of water waves after the wind field had been modified by the presence of the waves. He assumed the velocity profile in the air was steady and that the mean and periodic components in the wind were separately two dimensional though not necessarily parallel. The waves were assumed not to modify the mean wind field. Turbulence was included only insofar as the mean profiles suggested for use in the model were those common to turbulent rather than laminar flows. The logarithmic profile was considered the most applicable to prediction of ocean wave development.

Laboratory and field investigations showed that Miles' theory, while better than its competitors, consistently underestimated the growth rates of waves. Shemdin (1969) compiled several observers' results and compared them with his own. He concluded, in agreement with Phillips (1966) and others, that the omission of turbulent fluctuations and second order products of the wave perturbations was a major reason for the failure of the theory to estimate correctly the rate of energy transfer.

Experimental work continued, while other investigators turned to the task of including the neglected effects in a more general theory. The introduction of turbulence into a model always brings with it the problem of closure. The averaged equations for any quantity in a turbulent flow always contain correlations of one order higher, i.e., the equations for the mean flow contain the double velocity and pressure velocity correlations, those for the double velocity correlations contain triple velocity correlations and so ad infinitem. Most of the expansions on Miles' work thus settled down to introducing turbulence into the equations, choosing a closure scheme, and solving the resulting equations to see if anything believable resulted.

In order to solve a set of differential equations, one must have boundary conditions. For typical models such as those derived by Hussain and Reynolds (1970), Manton (1971), and Merceret (unpublished) it is necessary to specify boundary conditions at a surface and at infinity or another surface for both the mean flow and the perturbations. For solid walls, such as those used by Hussain in his experimental study, this poses no problem. For application to water waves under a semi-infinite atmosphere, however, it is impossible to establish sensible boundary conditions without knowing the answer before one begins the calculation. The models are created in order to determine the transfer of energy and momentum to the waves. If one knows the stresses at the surface exactly, the transfer can be computed. If not, then the boundary conditions cannot be specified.

A more profitable approach seemed to me to be to seek relationships among the variables in the region near the surface which would enable me to reduce the number of free variables and use these and the kinematic boundary condition to provide sufficient conditions at the surface. Like the closure schemes used in turbulence, this would require a combination of observation, dimensional analysis, and physical reasoning, and, like them, would give an approximate answer.

I had decided to make a systematic and careful field study of the lowest meter of the atmospheric boundary layer using hot-film anemometry to see whether there existed a detectable region of transition from a horizontally homogenous turbulent flow with a logarithmic profile to a region of different characteristics, possibly a laminar sublayer. I would also investigate the details of the transition region if I found it. If I could find a laminar sublayer and relate the flow in it to that outside I could use the laminar boundary conditions of Miles and our new information to solve the extended Miles model. Even if no laminar sublayer existed, I might find clues to useful relations for what did exist.

The study would begin on land and go to sea only if something useful resulted from the land-based work. Time and money were limited and we could not afford the risk and expense involved in working at sea until I was sure I had a chance of generating knowledge worth the cost of its acquisition.

That was what I planned to do. What was actually done was something more important.

While I was waiting for my equipment to be delivered, we received a visit from Professor Erik Mollo-Christensen of MIT, who presented a lecture at a Civil Engineering seminar. His lecture cast doubt on the whole framework of assumptions underlying the Miles theory and in private discussion he suggested the experiments I finally decided to perform.

Much of what Dr. Mollo-Christensen presented of the work of his group has not yet been published. The material here is from their published work together with what Dr. Mollo-Christensen suggested to me.

If one goes to sea in search of logarithmic velocity profiles to substitute into Miles' equations, one finds them. Disturbingly, though, the roughness parameter z_o seems to depend strongly on the wind speed and on the properties of the surface in a way which Ruggles (1970) suggests is a function of the generation mechanism. The data of Barger *et al.* (1970) support Ruggles' hypothesis, as do those of Mollo-Christensen (1970). A more detailed discussion of these data will be presented in Chapter II.

If the parameters of the profile depend on the generation of waves at the surface, one cannot assume a profile prior to computing the growth rate of the waves as required for Miles' theory and those models currently derived from it. The search for proper boundary conditions must wait until we've determined whether we yet have a proper set of averaged field equations. If Ruggles is right, the best available theories explaining the generation of waves by turbulent wind are wrong in principle and effort should be directed from expanding on them to devising a more correct, fully interacting model.

A major reason that the significance of the MIT work has been less appreciated than one might expect may be that there has been nothing with which to compare it. The variation of z_o with wind speed might be a function of the geometry of the boundary rather than its mobility. Wind tunnel measurements are not adequate because of the large difference in Reynolds number between laboratory and field situations. The bursts of high frequency turbulence reported by Mollo-Christensen (1970) associated with rapid changes in profile parameters might be causing the changes rather than occurrences at the surface.

When I discussed my proposed program with Dr. Mollo-Christensen, he agreed that our instrumentation and site were excellent to provide the supporting data to confirm or confute his group's work. Dr. Mollo-Christensen agreed that this would be a more fruitful use of our limited resources so I altered my plans accordingly.

II. THE STUDY

The possibility that the mean wind profile is not independent of the wave field is not original with Ruggles, but earlier papers imply a general belief that any variation of roughness length will be a smooth one as the wind speed increases, Priestley (1959), Kraus (1967), or at least piecewise smooth with a single region of transition where boundary layer separation over the waves begins, Bole and Hsu (1967). The data of Ruggles (1970) indicate the reality to be more complicated.

Ruggles fitted data from nearly 300 runs taken at sea with fetches greater than 26 miles to

$$\ln z = \frac{k}{u^*} U(z) + \ln z_o$$

where

z is the height above the reference level,

k is Von Kármán's constant,

U is the mean wind speed,

u^* is the friction velocity, and

z_o is the roughness length.

Table 1 displays the surprisingly large number of close fits he obtained. For these data the roughness length and friction velocity behaved in an unexpected manner, Fig. 1, Fig. 2. Note that the large ranges of u^* for a given wind speed at

Correlation coefficient	Number of samples
1.00	86
0.980-1.00	106
0.950-0.980	59
0.920-0.950	26
0.890-0.920	11
0.860-0.890	2
0.830-0.860	3
0.800-0.830	2
0.740-0.800	0
0.700-0.740	4

Table 1. Correlation with logarithmic profile from Ruggles (1970)

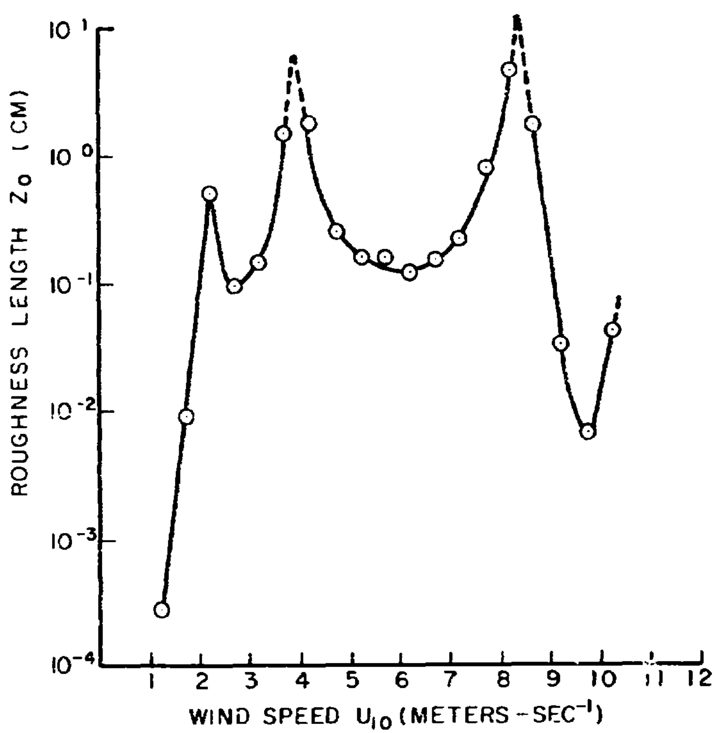

Fig. 1. z_o as a function of U_{10} from Ruggles (1970)

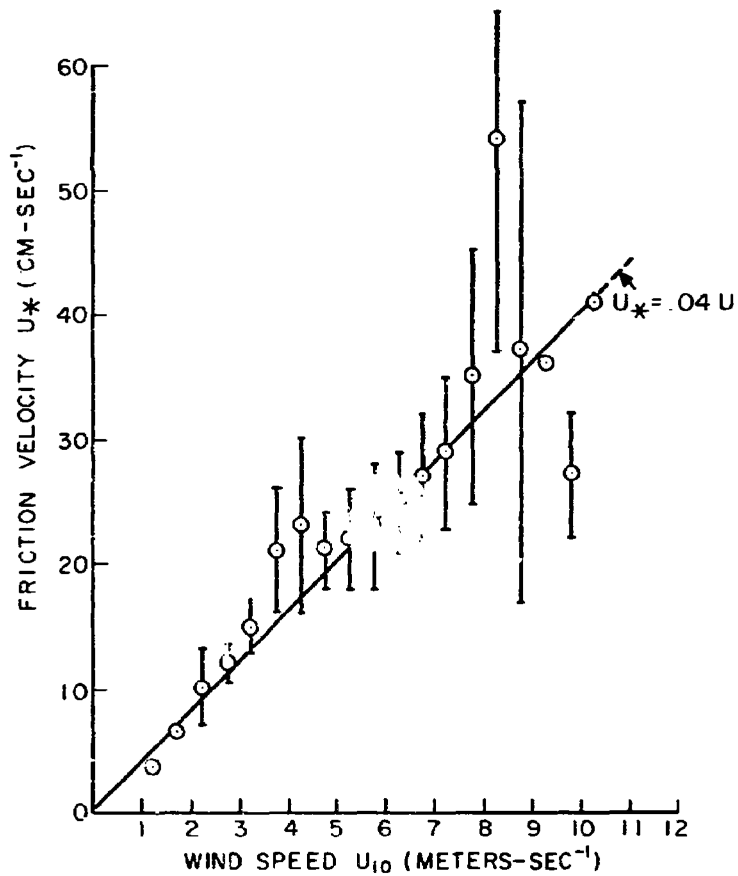

Fig. 2. u* as a function of U_{10} from Ruggles (1970)

10 meters, U_{10}, occur where the peaks in the z_o plot occur. The multiple peaks disappear in the presence of an oil slick, Fig. 3, Barger *et al.* (1970). The large ranges indicated for u* do not represent values of u* distributed over the whole range. Rather, the values of u* cluster at the extremes of the range, and the value appearing in a particular profile depends on the ratio of presence to absence of high frequency bursts in the turbulence, Mollo-Christensen (1971).

The MIT group interpret these data as showing wind-speed dependent momentum interchange between the wind field and the wave field. When large transfer occurs the surface of the sea roughens as capillary and small gravity waves are generated on the backs of the waves constituting the swell. Thus z_o increases. At the same time the transfer of momentum changes the values of the Reynolds stresses, thus changing u*. The burst structure for the high frequency turbulence coincides with a similar phenomenon on the water surface where small wavelets are seen to be generated in patches which suddenly appear and disappear, Kinsman (personal communication).

The burst structure has been observed in the atmosphere over land, Haugen, Kaimal, and Bradley (1971), and in the laboratory, Kim, Kline, and Reynolds (1971) but the variation of roughness length with wind speed has been observed only over yielding surfaces such as the sea or very long pliant grass, Priestley (1959). The roughness length over flat land seems

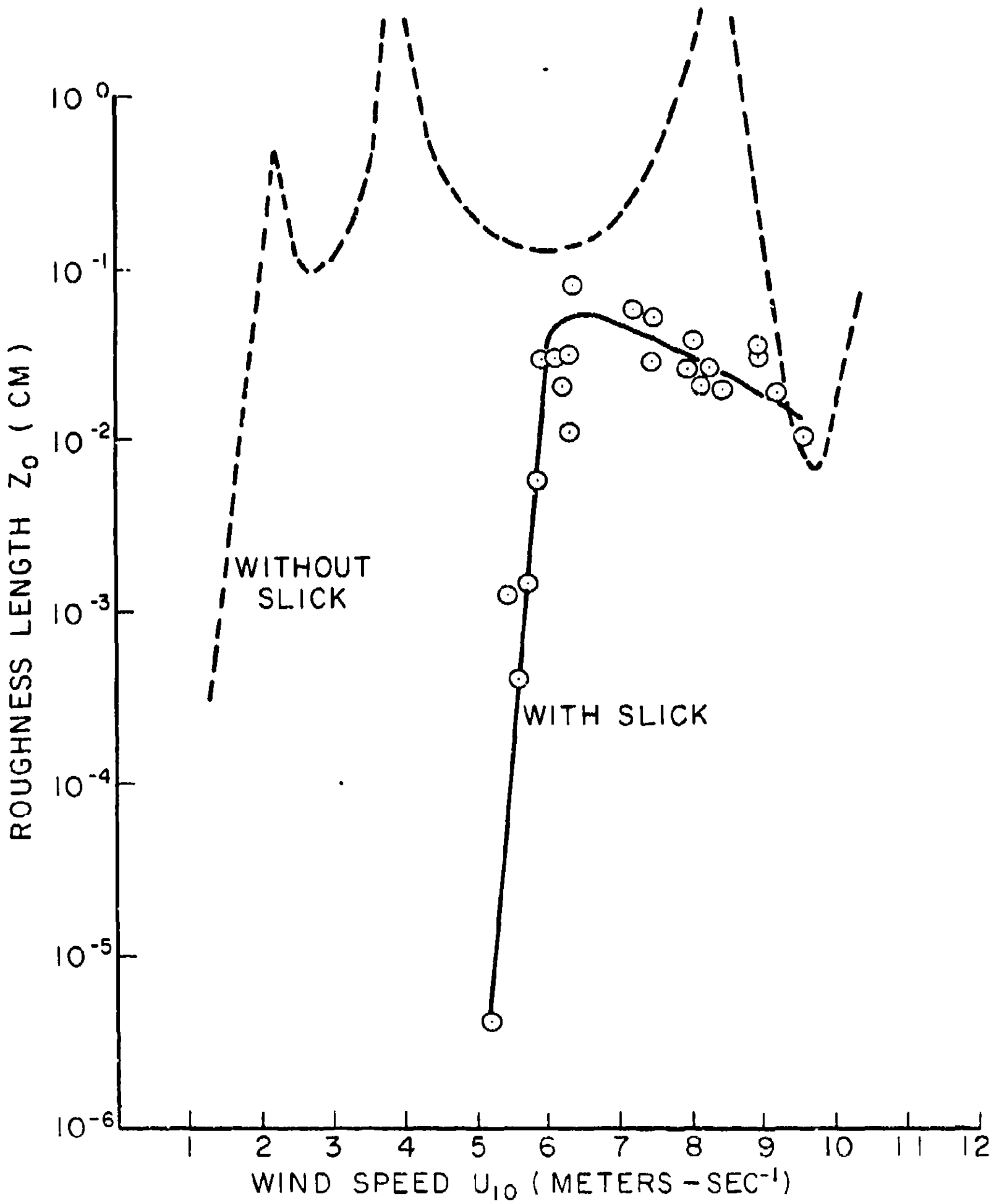

Fig. 3. z_o as a function of U_{10}

from Barger *et al.* (1970)

independent of wind speed, Priestley (1959), Lumley and Panofsky (1964). The value of z_o as a function of wind speed has not been systematically investigated over a periodic fixed surface, as far as we are aware, outside of the laboratory; thus it is still possible that Ruggles' data may be indicative of a shear instability in the wind flow rather than of occurrences at the surface.

The present experiment is designed to test the hypothesis that the surface configuration is alone responsible for the value of z_o, even over a corrugated surface, and to examine the burst structure as it relates to the value of u^* in logarithmic profiles.

In order to get the strongest possible connection with Ruggles' work, an experimenter should use similar instruments in a similar configuration and process his data in the same manner as Ruggles. Of course, additional information beyond what Ruggles obtained should be used when it is available to illuminate the problem and care should be taken to ensure that the results are not a fiction of the instruments or data handling methods. The MIT experiments used light-interrupting cup anemometers for mean wind speeds at higher levels and hot-film anemometers at lower levels for mean winds and turbulence levels. We had ordered the same kinds of instruments, which will be described in a later section. The field site should be one periodically corrugated with a long unobstructed fetch. Such a site was available to us and will be described in the next section.

In the experiment we would have to do the following:

1. Obtain velocity profiles
2. Select those which are logarithmic with a correlation of 0.9 or better
3. For these profiles plot z_o *vs.* U_{10} and note the presence or absence of peaks such as Ruggles found
4. Plot u* *vs.* U_{10} and look for regions of high variance and, if they exist, correlate them with such peaks as show up in the z_o plot
5. Look for bursts of high frequency activity at each level and determine whether they occur simultaneously, sequentially, randomly, or not at all
6. If bursts occur nearly simultaneously, reduce portions of the record during bursts and the remainder, separately fitting them to logarithmic profiles.

The goodness of fit should yield information on the rate of adjustment of the profile while the values for z_o and u* may be used to determine whether u* correlates with the burst structure and whether z_o is a function of the burst mechanism. If the bursts occur sequentially with the same ratio of time occupied by bursts to that of the total record obtaining at each level then this method would still be used, but additional information would be gained from studying the lag time between levels. If the bursts occur randomly at each level or not at all, it would tend to indicate the phenomenon is not of sufficient depth, or frequency respectively, to be a major determining factor in the shape of the profile.

If the burst structure is observed, and if z_o is not a function of the wind speed or the burst structure but u* is dependent on both, then the speculations of the MIT group are well founded and we need to reconsider our acceptance of the prescribed-profile models accordingly. If otherwise, then some investigation into other mechanisms for the variation of the profile parameters would be indicated.

III. THE SITE

I preferred a field site in the Delaware Valley as close to Newark as could be found because my laboratory and data analysis facilities were in Newark, Delaware at The University of Delaware's College of Marine Studies. I needed a periodically corrugated, relatively unvegetated surface with a long unobstructed fetch in the direction of the predominant wind. The experiment would require a wind relatively steady in direction and mean magnitude over periods of the order of tens of minutes. Thus the time of the year for the work and the alignment of the fetch were determined by the climatology of the Delaware Valley region.

The winds steadiest in direction and of sufficient speed to cover the range of interest occur in Delaware from late October to early April with the months February and March providing the best conditions, Mather (1968). During these months and during early April, the prevailing wind is from the west to the north with northwest winds occurring nearly 30% of the time. Wind roses for March and April for the station closest to our site are shown in Fig. 4. Because our equipment arrived in late February we operated only during the period mid-March to mid-April. The actual winds were quite satisfactory during this time, being from the desired direction

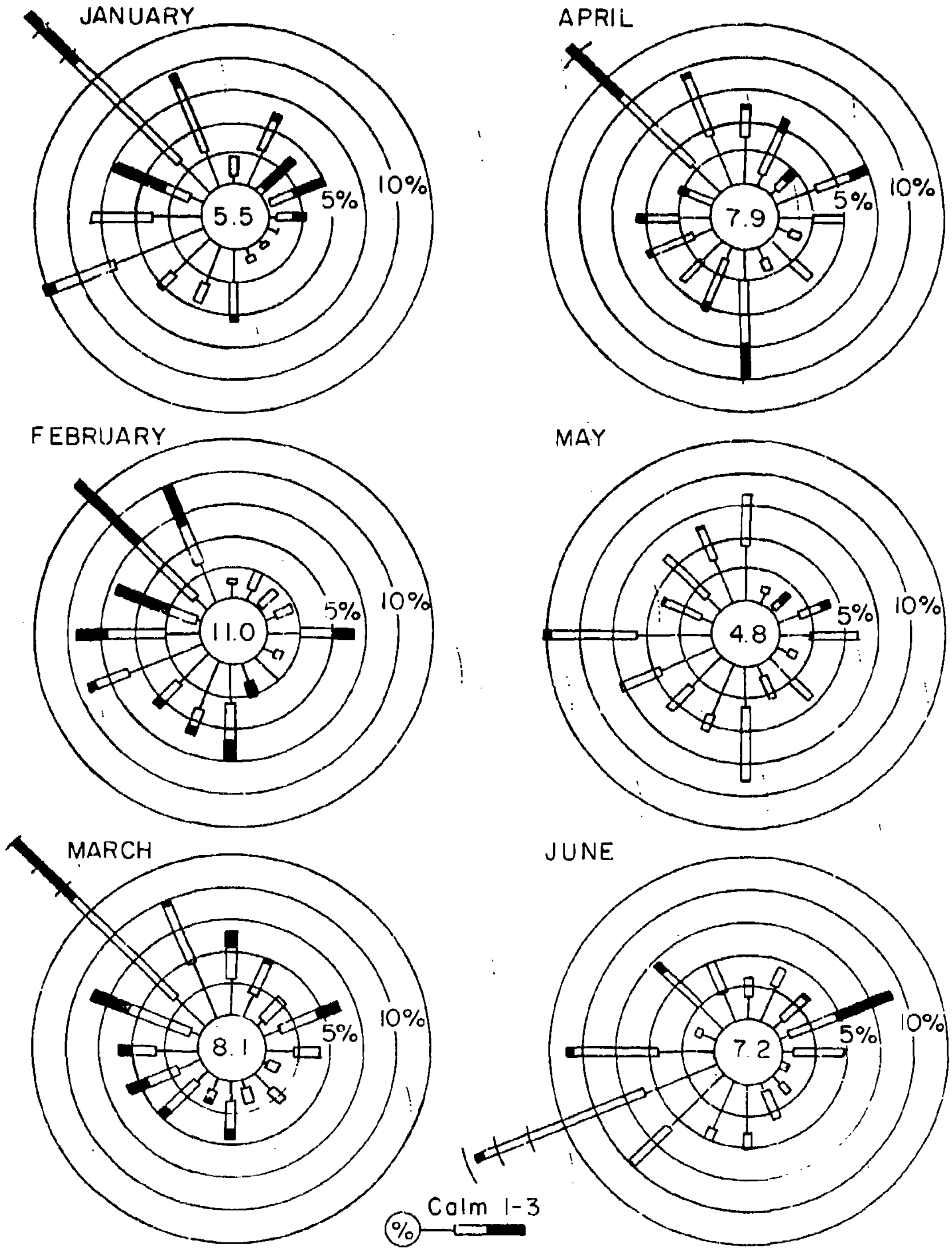

Fig. 4. Wind roses for January through June at Delaware City from Mather (1968)

over a suitable range of speeds.

The vicinity of The University of Delaware abounds in small airports and plowed fields. A plowed field is suitably corrugated while an airport usually has an adequate fetch in the direction of the prevailing wind. We were fortunate to find a plowed field adjacent to a well kept but little used grass airstrip, the owners of each of which were willing to tolerate a clutter of equipment, a tower, and interloping scientists on their property. The airport's windsock was a bonus. From it we could estimate the steadiness of the wind direction. Figure 5 shows the site which is located near the Delaware-Maryland border in Elkton, Maryland. On Fig. 6, note the location of the site and of Delaware City for which the wind roses have been presented.

In the direction of the predominant wind, northwest, the fetch is unobstructed and the surface almost level for more than 1 km. There were no obstructions in the semicircle from SW through NW to NE closer than about 900 meters except for several small trees and a number of two story farm buildings due west at about 550 meters, and a stand of trees slightly east of north at about 480 meters. Downwind obstructions included a two story house and some one story aircraft hangers about 360 meters away to the SSE and SE, respectively, and a stand of trees due east at about 500 meters. Otherwise, the

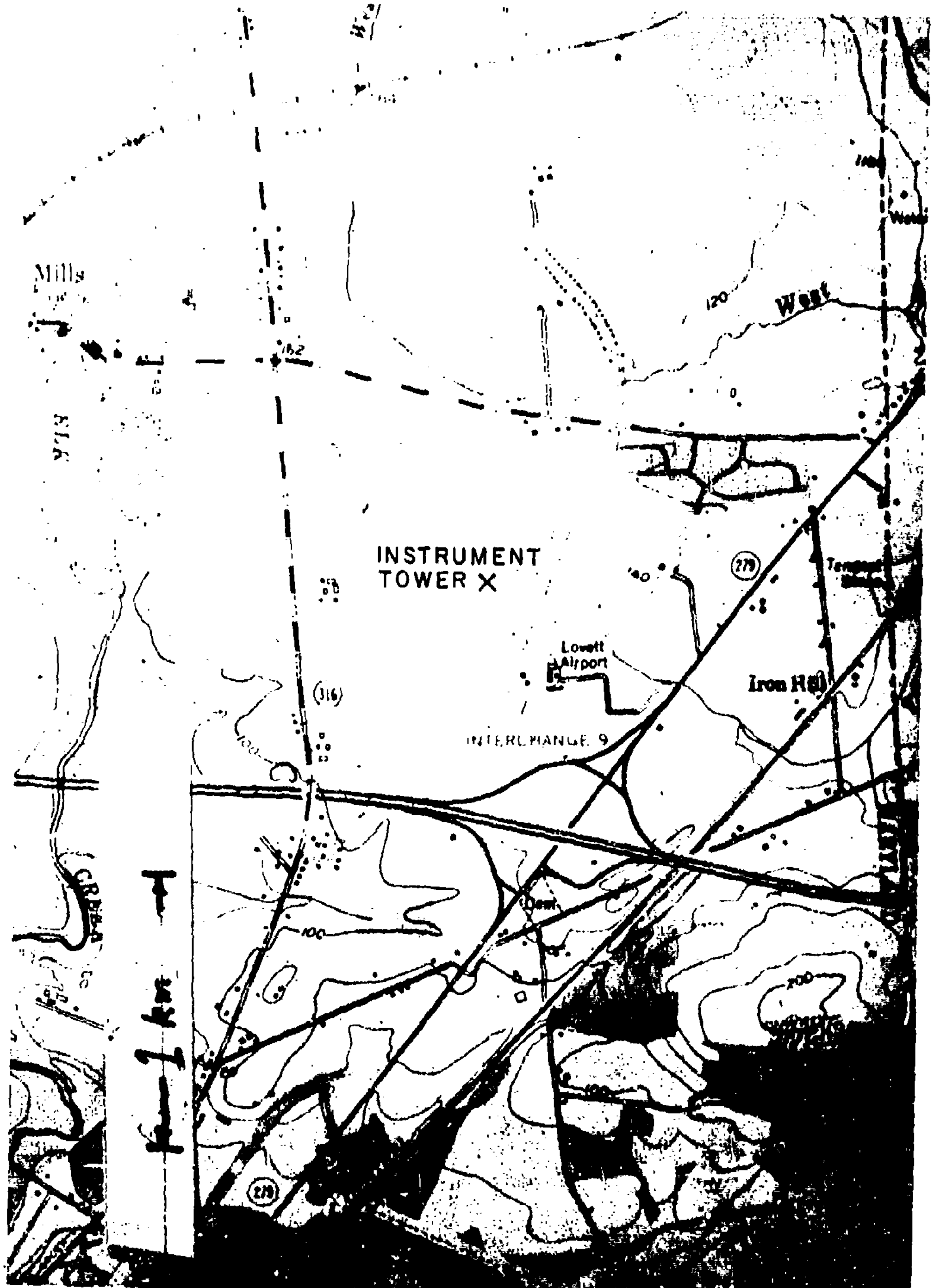

Fig. 5. The field site

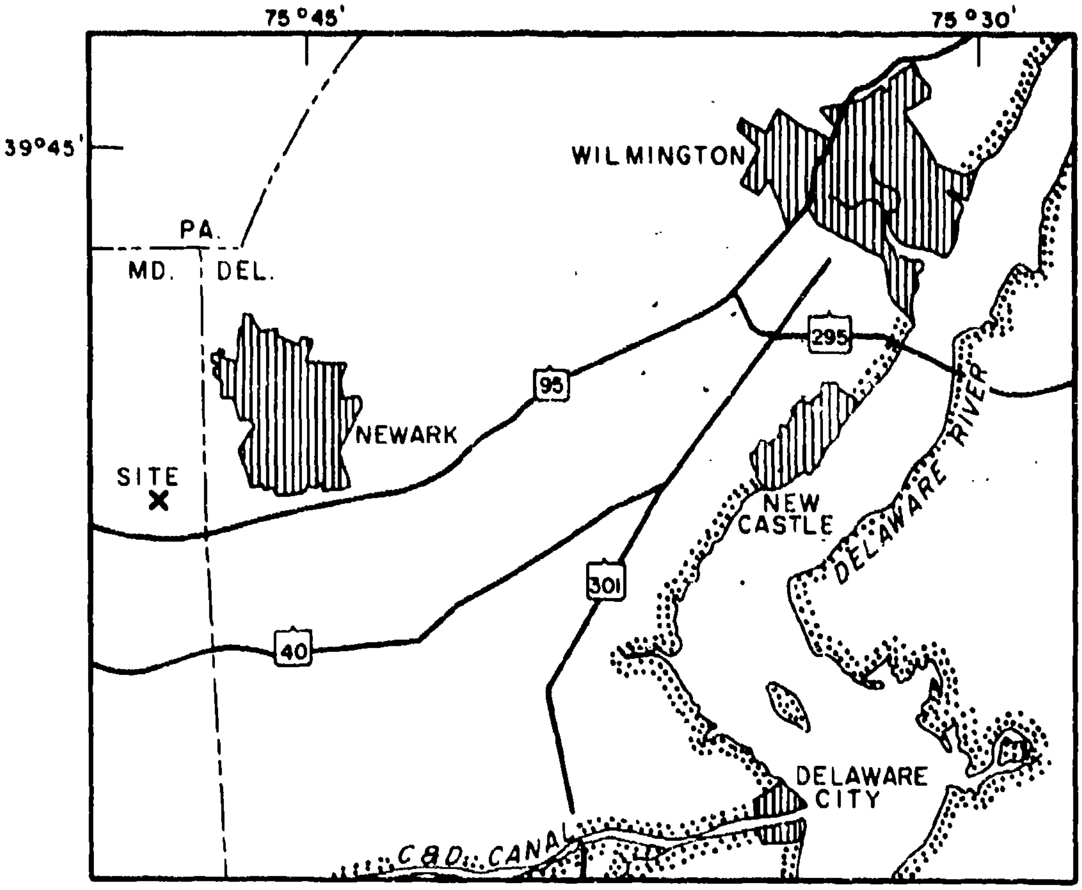

Fig. 6. Northern Delaware and nearby places

downwind fetch was unobstructed for at least 700 meters in all directions.

The site is plowed from the farm buildings to the edge of the airstrip. The plow contours have the approximate form of an unsymmetrical square wave with an amplitude of 10 cm and a wavelength of 90 cm, Fig. 7. The furrow crests run nearly east-west. Cornstalks ranging from a centimeter to perhaps 30 cm high and 1-3 cm in diameter punctuate the surface every meter or so, but many of them have been flattened against the ground so that those remaining form a random and relatively sparse pattern. The soil was firm even after heavy rain, and water did not appear to collect anywhere in the field during the two months we used the area; nor was the field at any time snow or ice covered.

The site is ideal for this research. Its proximity to our laboratory made it possible to test, repair, and reinstall equipment during a day's run. It enabled us to operate on very short notice when the weather was right. The steady wind and long unobstructed fetch aligned nicely, while the nature and contours of the surface were as if made to order.

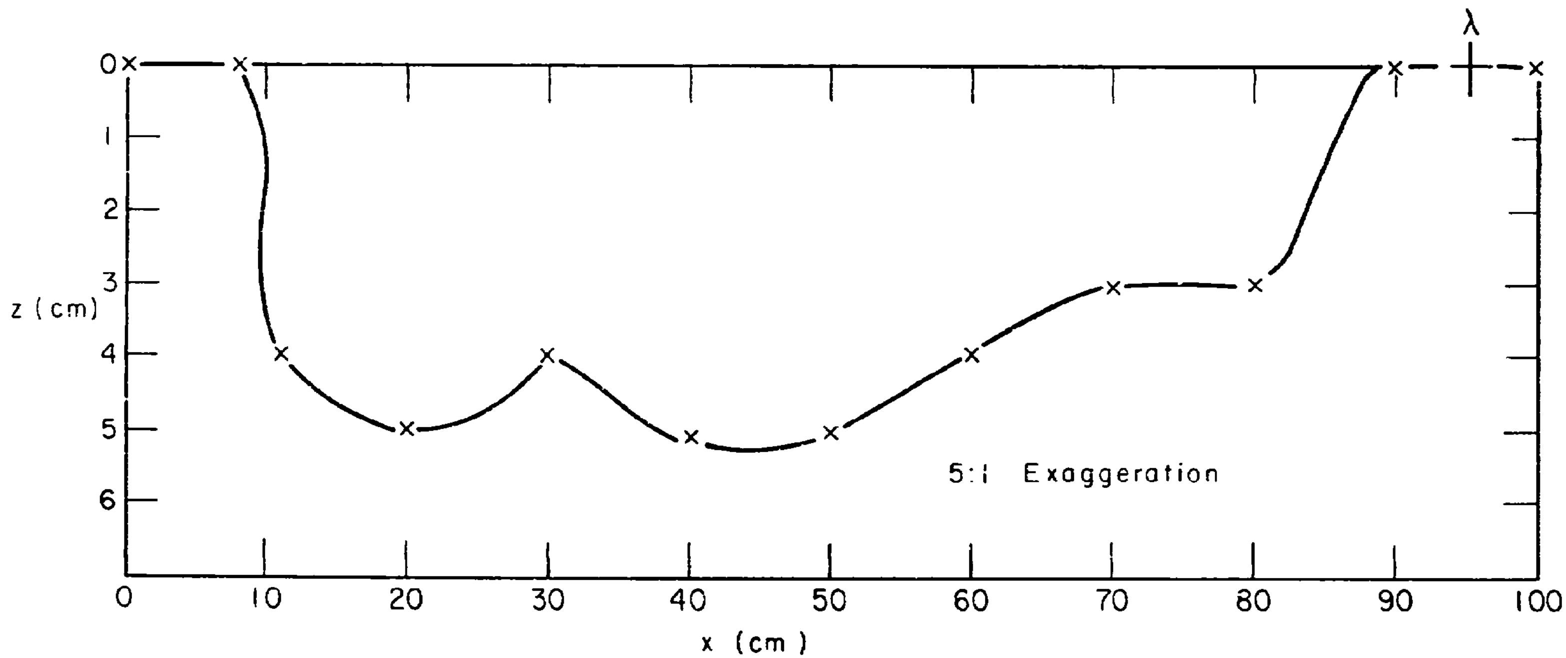

Fig. 7. Contour of a typical furrow

IV. THE INSTRUMENT SYSTEM AND ITS FIELD INSTALLATION

The wind instruments were cup anemometers and hot-film anemometers. The cup anemometers, including data registers, were C.W. Thornthwaite Associates Wind Profile Recording System Model 106. The anemometer cups are of light-weight plastic reinforced with aluminum rings while stainless steel tubing forms the spokes and the hub is of aluminum. The entire cup assembly weighs only 7 grams. The anemometer shaft is made of hardened stainless steel. Miniature ball bearings are used. A shutter mounted on the shaft interrupts a light beam from a 3-volt grain-of-wheat lamp housed in the base of the anemometer tee and breaks a beam of light focused on a photocell once for every revolution of the cup assembly. After amplification the output of this photocell operates an electromechanical counter directly. No relays are used in the Wind Profile Recording Systems. One count registers on the counter for each revolution of the cup assembly. The counters are mounted on the front panel of the cabinet for ease in reading. The anemometers in our set were factory calibrated and matched to within ±0.2%. The calibration curve for the system is shown in Fig. 8. The specifications supplied by the manufacturer and confirmed at Delaware are shown in Table 2.

The response of the cup anemometers to tilt is essentially flat within 45° of horizontal, see Fig. 9, Thornthwaite, *et al.* (1959), and the system acts like a low pass filter for small

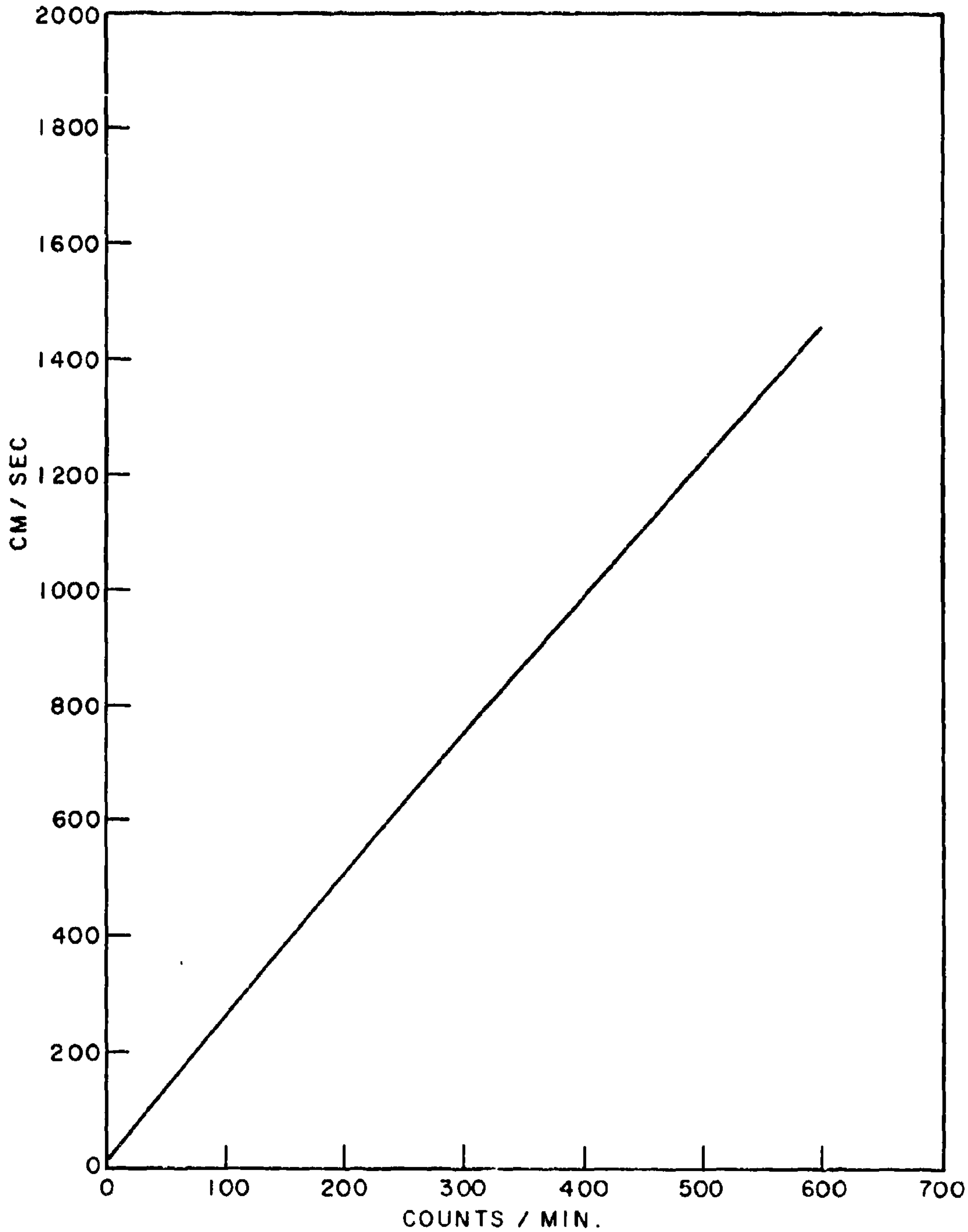

Fig. 8. Cup anemometer calibration from Thornthwaite *et al.* (1959)

WIND SPEED RANGE:

0 - 32 mph, 0 - 1450 cm/sec

STARTING SPEED:

less than 0.20 mph (8.94 cm/sec)

DISTANCE CONSTANT:

83.3 cm in horizontal flow

READOUT RESOLUTION:

0.1 cm/sec (1 hour profile)

POWER SUPPLY:

1 - 12 v storage battery
1 - 1.3 v mercury cell

INDICATION:

electromechanical register

ANEMOMETER CUPS:

conical, plastic, 2 in diameter; assembly weight, 7 grams (0.25 oz)

TRANSMITTER HOUSING:

chrome plated brass mounted on 3/8 in o.d. arms 12 in long; total weight of transmitter 156 grams (5.5 oz); upright cup assembly support, 3/8 in o.d.; height 14 cm; maximum interference dimension viewed by the wind, 1/2 in

CABINET:

9"H × 8-1/8"W × 12"D, 3.63 kg (8 lbs)

Table 2. Manufacturer's specifications for cup anemometer system supplied by C.W. Thornthwaite Associates

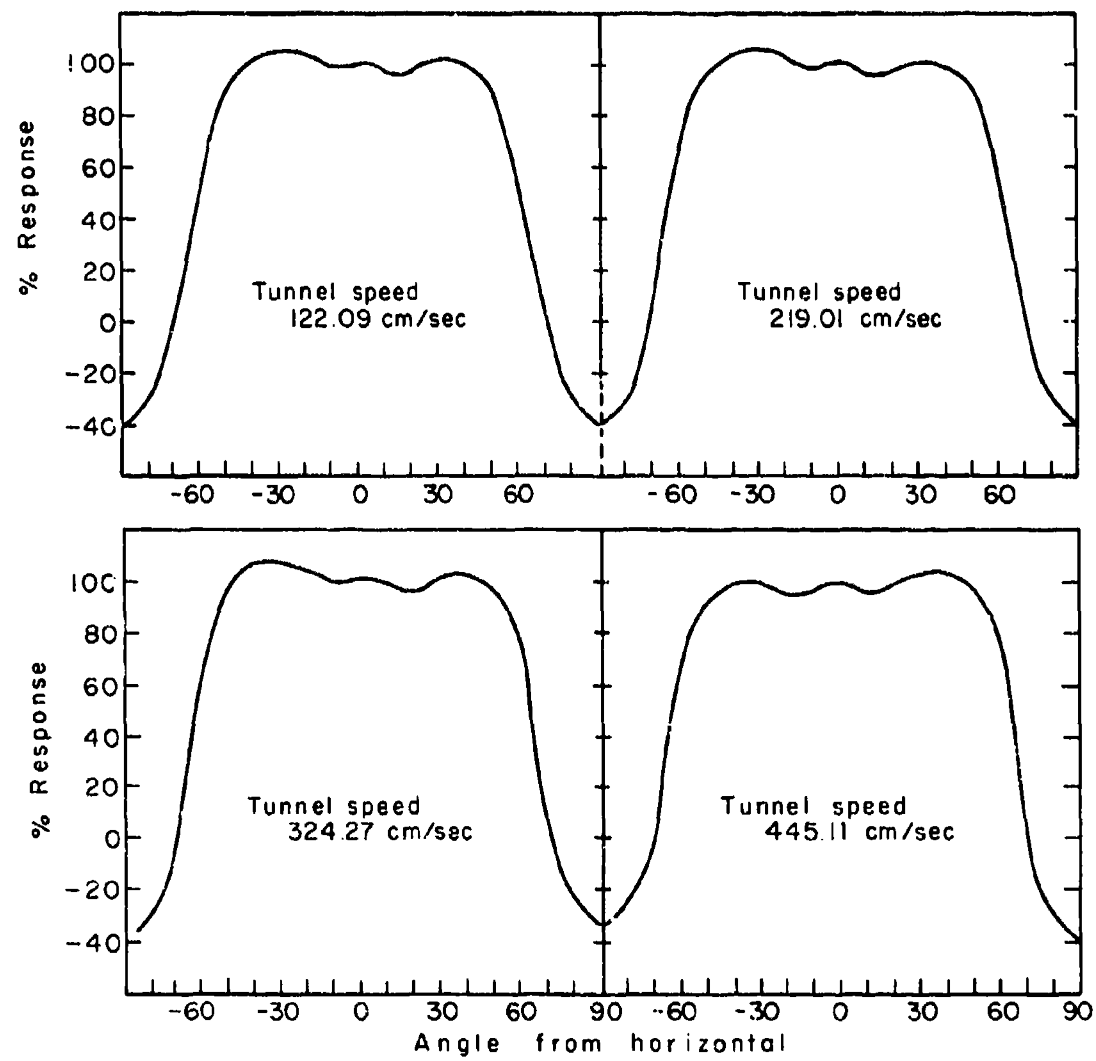

Fig. 9. Directional response of cup anemometers from Thornthwaite *et al.* (1959)

scale fluctuations, see Fig. 10, Thornthwaite, Superior, and Mather (1961). For our system, the 3 db response point occurred at about 4 meters with essentially full response for scales larger than 20 meters.

The hot-film sensors were DISA 55A81 quartz-coated wedge shaped probes. DISA 55D05 battery operated constant temperature anemometers and 55D15 portable linearizers were used. Films were preferred to wires because they are more rugged and relatively insensitive to weather, Merceret (1970). We chose to linearize the system for two reasons. The range of winds expected and the turbulence level anticipated were large enough that linearization should significantly contribute to accuracy, and the ability to suppress the zero-wind bridge voltage would allow better use of the limited dynamic range of the recording system.

The probes were operated at about 200 C. At this temperature, in wind fields of the kind expected, the frequency response of the system is essentially flat to beyond 200 Hz, with the 3 db point well beyond 1 kHz, Merceret (1969), more than adequate for the proposed measurements, see Fig. 11. The directional response of the films is not so forgiving as that for cups, Merceret (1968), and a steady wind and careful alignment of the probes were necessary for high accuracy. Factory specifications for the anemometers and linearizers are presented in Tables 3 and 4. The specifications for the anemometers were confirmed, Merceret (1968), (1969), while those for the linearizers were

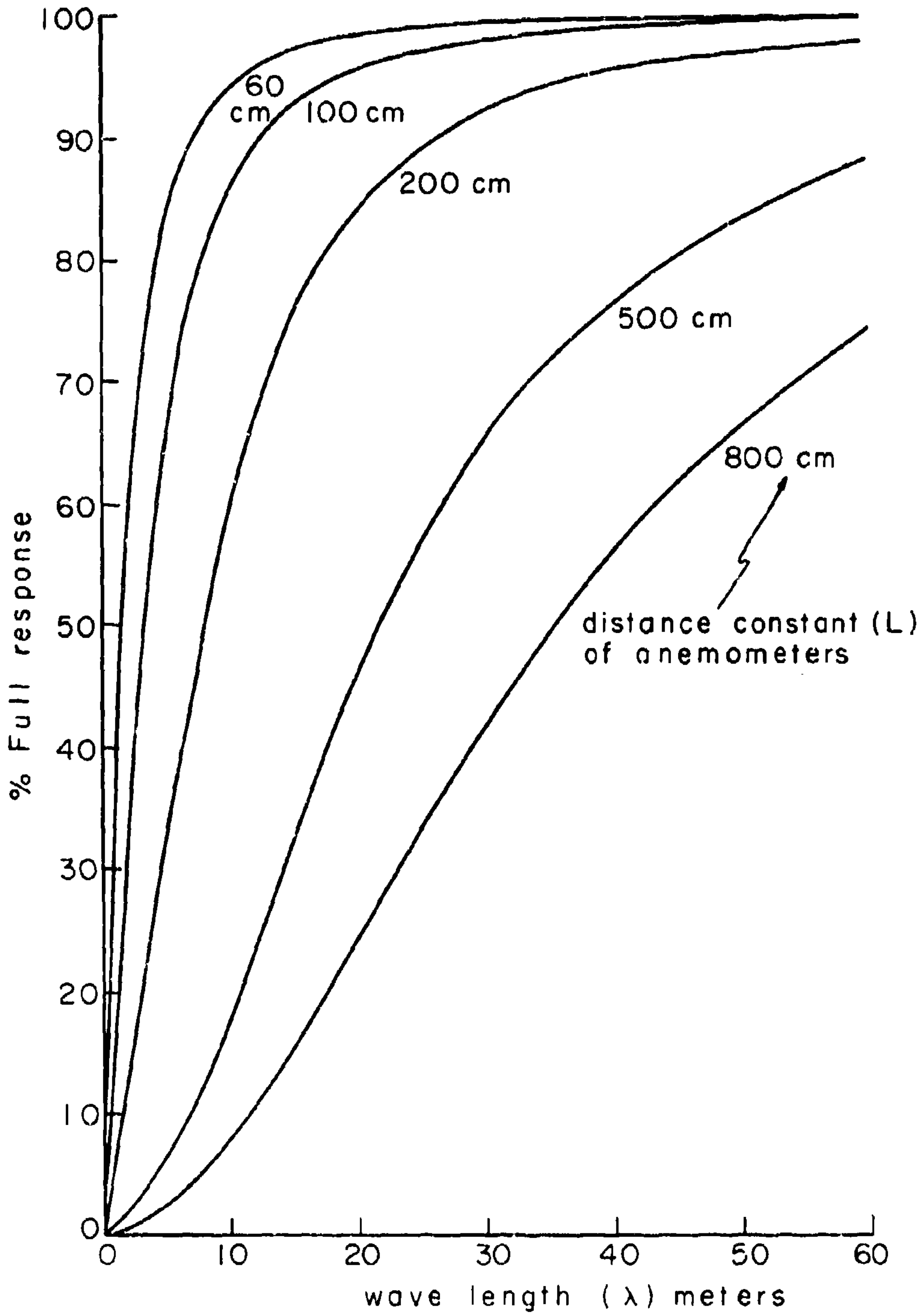

Fig. 10 Wind fluctuation wave-length *vs.* response of cup anemometers

from Thornthwaite, Superior, and Mather (1961)

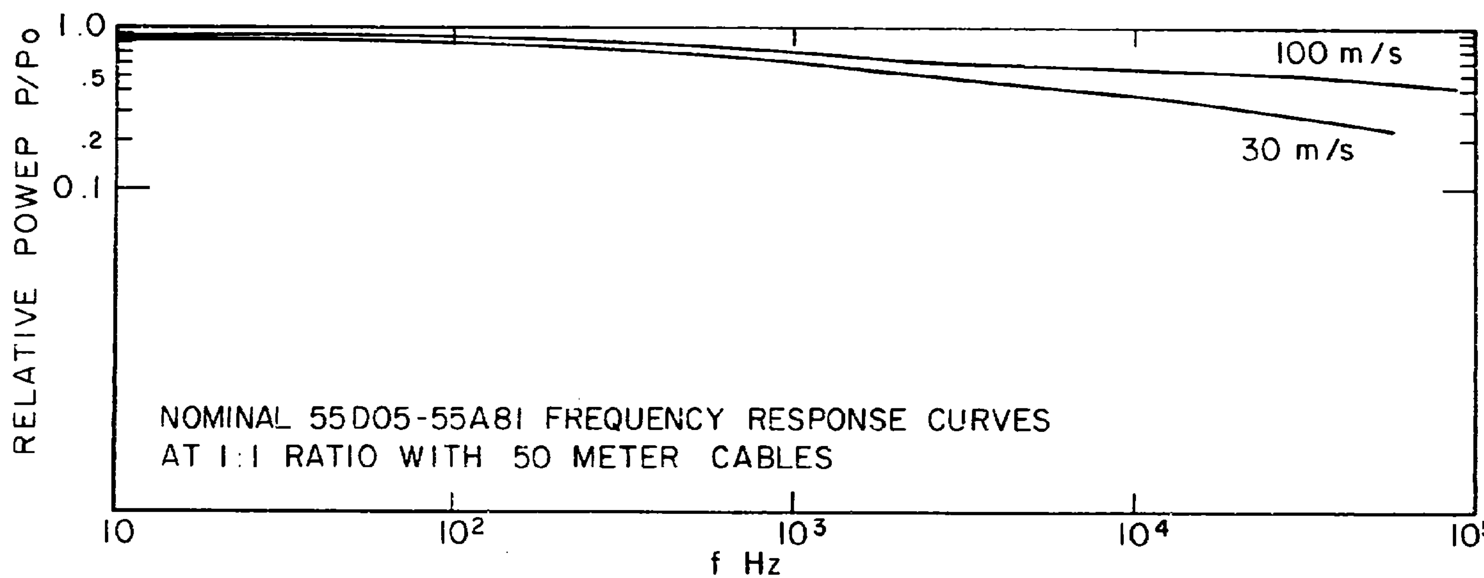

Fig. 11. Frequency response of hot-film anemometers from Merceret (1969)

TYPES OF OPERATION:

10:1 bridge ratio and 1:1 bridge ratio

PROBES:

hot-wire or hot-film types
note: hot-film probes normally require an external resistor

PROBE RESISTANCE RANGE:

built-in bridge arm: 2.4 to 13.0 ohms in 10 steps
external bridge arm: 1 to 50 ohms

NOISE LEVEL:

approximately 0.8 mV_{rms} at zero flow velocity and 50 kHz bandwidth (the noise level is proportional to the bandwidth)

OUTPUT VOLTAGE:

approximately 1 to 7 volts at full flow velocity

OUTPUT IMPEDANCE:

approximately 500 ohms

FREQUENCY RANGE:

10:1 bridge ratio: 0 - 50 kHz. The upper frequency limit depends on the conditions of measurement and on the type of probe used

1:1 bridge ratio: 0 - 100 kHz. The upper frequency limit depends on the accuracy of the compensating cable, on the conditions of measurement, and on the type of probe used

POWER SUPPLY:

built-in, two HELLESENS Type H-10 9-volt batteries or equivalent and six Type BA-30 1.5-volt dry cells or equivalent, for instance HELLESENS Type VII-36

Table 3. Manufacturer's specifications for hot-film anemometer system supplied by DISA S & B (continued on page 30)

Table 3. continued from page 29

EXTERNAL POWER SUPPLY:

extra bridge power may be supplied (maximum 20 volts DC)

AMBIENT TEMPERATURE:

0 to +45 C

CIRCUIT:

fully transistorized (silicon transistors)

DIMENSIONS:

62 mm high, 212 mm wide, 220 mm deep

WEIGHT:

2.4 kg inclusive of batteries

BASIC TRANSFER FUNCTION:

$$V_{out} = K(V_{in} - V_{ino})^m \text{ and } V_{out} = K\,V_{in}^m$$

EXPONENT (m):

2 - 3 - 4 - 5 - 6 (±5%)

INPUT RESISTANCE ($R_{in} = V_{in}/I_{in}$):

850Ω to 5 kΩ

MAXIMUM INPUT VOLTAGE:

30 volts

OUTPUT VOLTAGE RANGE:

maximum output voltage better than 3.5 volts
DC output voltage can be measured with built-in meter
meter range: 0 - 3 volts
meter accuracy: 2% of full scale

OUTPUT IMPEDANCE:

approximately 10 Ω
maximum load: 1 kΩ (or maximum output current: 4 mA)

OUTPUT VOLTAGE CHANGE PER DEGREE CENTIGRADE (AMB. TEMP.):

Typical	Maximum	
0.2% per C	0.5% per C	(at m = 2 and 3)
0.3% per C	0.6% per C	(at m = 4)
0.4% per C	0.8% per C	(at m = 5)
0.5% per C	1.0% per C	(at m = 6)

OUTPUT VOLTAGE STABILITY:

ΔV_{out}/10 hours at constant temperature

maximum 0.05 volt with battery supply
maximum 0.001 volt with external stabilized power supply

Table 4. Manufacturer's specifications for linearizers supplied by DISA S & B (continued on page 32)

Table 4. continued from page 31

TYPICAL OUTPUT NOISE:

1 mV_{rms} at full bandwidth

0.2 mV_{rms} at 10 kHz

DIMENSIONS (HWD) IN MILLIMETERS:

62 × 212 × 280

WEIGHT:

1.8 kg

POWER SUPPLY:

built-in: twelve HELLESENS VII 28 1.5-volt dry cells or equivalent (e.g. MATSUSHITA ELECTRIC UM3D, Mallory Radio Penlight M15R)

AMBIENT TEMPERATURE RANGE:

0 to +45 C

TYPICAL UPPER FREQUENCY LIMIT (3 db): m = 3:

V_{out} DC volts	3	2	1.2	0.5
kHz	70	100	175	240

confirmed during this study except as will be noted in Chapter V.

The wind instruments were mounted several ways. The cup anemometers were always attached to an 8-meter tri-sectioned mast of two inch aluminum irrigation pipe guyed so as to avoid interference from the wakes of the guy wires. The attachment was made using crossarms of 3/4 in square aluminum stock and U bolts, as is conventional in mounting TV antennas. Each cup was about eighteen inches from the mast and positioned to the side of the upwind-downwind line to avoid aerodynamic interference from the mast, Fig. 12.

We had four cup anemometers in the array, the top three of which were at 4 m, 2 m, and 1 m above the top of a furrow except during the instrument checkout run during which the four cups were at 7.9 m, 3.9 m, 1.9 m, and 90 cm. The bottom cup was placed at the same height as the top film on every run to cross-check the instruments. This height was either 50 cm or 25 cm depending on the run.

The hot-film units were on separate mounts described in the next paragraph. There were three working channels available, the top one of which was always at 50 cm or 25 cm above the crest of a furrow. The remaining two probes were then located at two heights selected from the following: with a top of 50 cm; 25 cm, 12.5 cm, and 6 cm or with a top of 25 cm; 12.5 cm, 6 cm, 3 cm, and 1 cm. None of the data taken at the 1 cm

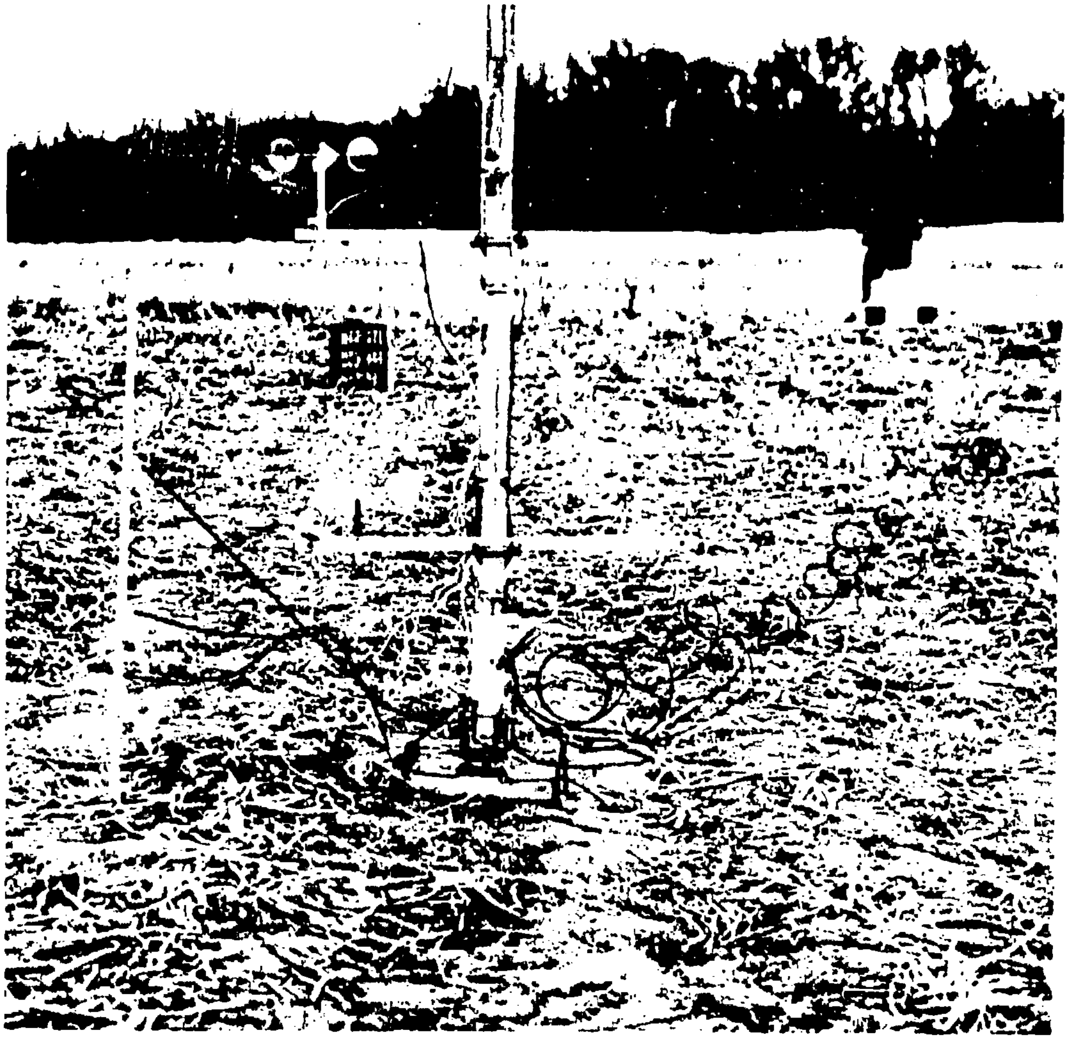

Fig. 12. Cup anemometer installation

position were recoverable but all of the data taken at greater heights were usable.

The hot-film anemometers were mounted on 18 in steel shafts attached to aluminum blocks which fitted onto 1/2 in wooden dowels. The dowels provided electrical isolation of each probe. These dowels were attached to the tower cross-arms for instrument cross checks and thereafter mounted in the ground beside the large tower as probe supports, Fig. 13.

In order to have a measure of the temperature distribution in the air near the surface, we installed two mercury in glass meteorological thermometers with radiation shields at heights from 0.20 to 2 m above the surface. These were read to the nearest 0.01 C at the beginning and end of each run.

The thermometer readings and cup anemometer counts were recorded on prepared forms with the time and date of the beginning and end of each run. The data from the hot-film systems were recorded on a Lockheed model 417 analog tape recorder and the date and time marked on each reel.

We used the Model 417 in a 4-channel FM record-playback configuration using a Lockheed storage cell for power. The tape speed most convenient for our work was 7-1/2 ips which gave us flat response from D.C. to well above 1 kHz while allowing enough tape for 30 minutes of data plus another 5 minutes of calibration signals on each reel. The manufacturer's

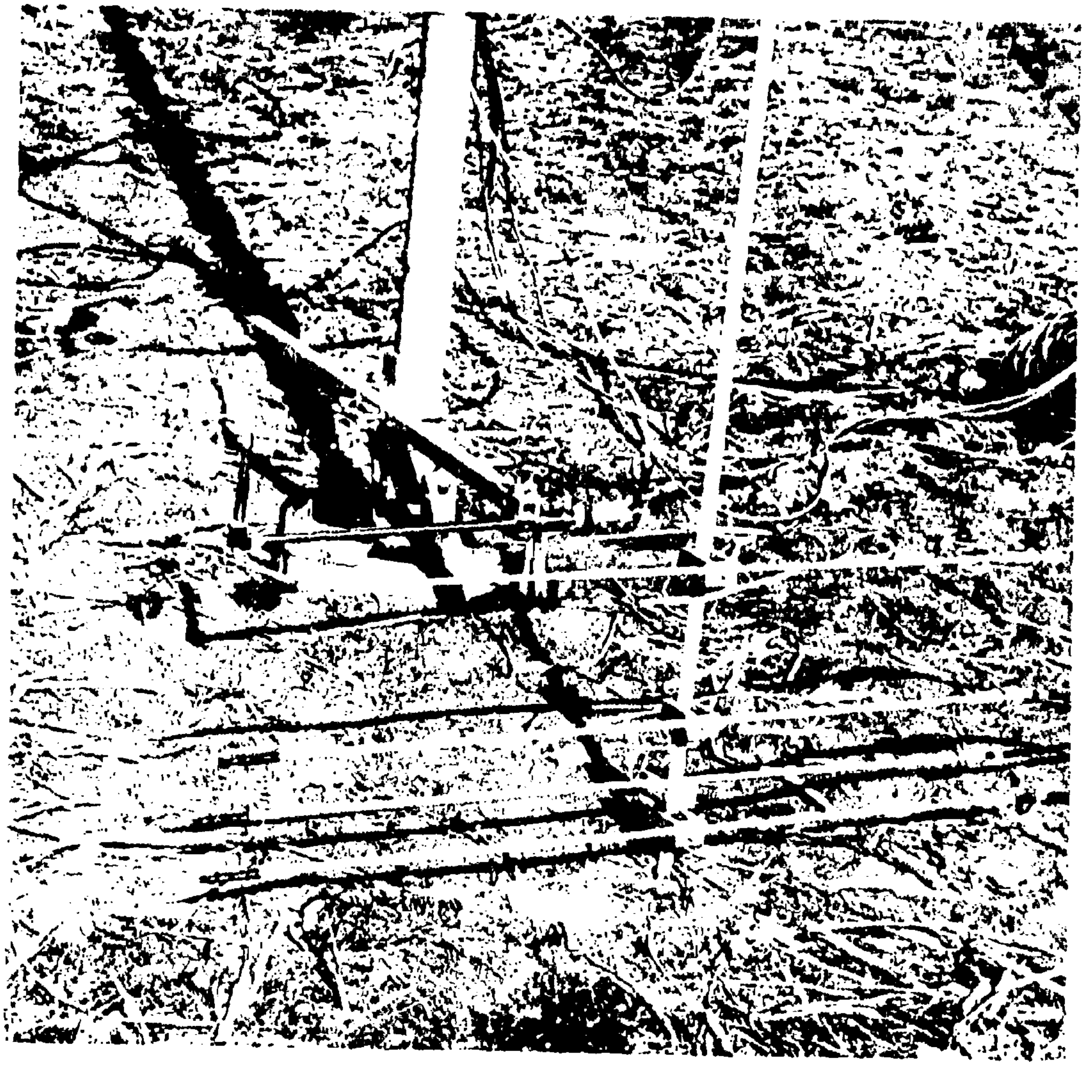

Fig. 13. Hot-film anemometer installation

specifications are presented in Table 5. A three to one voltage divider of precision resistors was used to step down the voltage from the linearizers to a value compatible with the limits of the recorder. This enabled us to run the 55D15's at full gain so there would be less probability of misadjusting the gain control than if we used an intermediate setting, and it allowed us to utilize the full dynamic range of both instruments.

1. GENERAL

TAPE SPEEDS: 7-1/2, 15, and 30 ips

TAPE DIMENSIONS: up to 3150 feet of 1/2 in polyester-backed recording tape can be accommodated on a 7 in reel

RUNNING TIME: 45 minutes at 7-1/2 ips for 1800 feet

START AND STOP TIME: acceleration to 7-1/2 ips, 5 sec maximum

FLUTTER: the cumulative peak-to-peak flutter as measured 95% of the time, will not exceed 0.8% at 7-1/2 ips

2. FM SYSTEM

RMS SIGNAL-TO-RMS NOISE: 40 db measured across passband of recorder at 7-1/2, 15, and 30 ips

HARMONIC DISTORTION: 1.5% total harmonic distortion measured at 1/2 cut-off frequency

A.C./D.C. LINEARITY: 1% of full scale at all speeds

DRIFT: 1.0% of full scale from 1/2 minute to 1 hour, at constant temperature of 68 F. 0.3% of full scale from 5 minutes to 1 hour, at constant temperature of 68 F

TEMPERATURE STABILITY: 0.05% per degree F from 32 to 120 F

INPUT SENSITIVITY: ±1.4 volt (1.0 volt rms) for ±40% deviation

INPUT IMPEDANCE: 20,000 ohms minimum over the passband

OUTPUT VOLTAGE: ±1.4 peak volts (1.0 volt rms) for full carrier deviation

OUTPUT IMPEDANCE: 1000 ohms maximum over the passband

OUTPUT LOAD: 10 K ohms minimum

Table 5. Manufacturer's specifications for tape recorder supplied by Lockheed (continued on page 39)

Table 5. continued from page 38

MAXIMUM DEVIATION: ±40%

CENTER FREQUENCY AT 7-1/2 IPS: 13,500 Hz

FREQUENCY RESPONSE AT 7-1/2 IPS: 0 to 2,500 Hz

3. ENVIRONMENTAL AND PHYSICAL SPECIFICATIONS

OPERATING TEMPERATURE RANGE: 0 to 45 C

HUMIDITY: up to 99% (without condensation)

ORIENTATION: operates in any position

SIZE, STANDARD CASE: 13-15/16" × 15-3/16" × 6-3/8", exclusive of handle

WEIGHT, STANDARD CASE: 29 pounds, including self-contained battery

POWER REQUIREMENT: approximately 13 watts at a nominal 17.5 volts

V. THE CALIBRATION AND USE OF THE SYSTEM

We checked the factory calibration of the cup anemometers and calibrated the hot-film systems in the 12 × 18 inch test section of a low turbulence wind tunnel at The Johns Hopkins University, see Kellogg (1965), using a pitot-static tube and liquid micro-manometer as the reference instrument for velocity.

The manufacturer's specifications for the cup anemometers were correct to within about 1% of the indicated flow at velocities above the starting velocity as presented in Fig. 8.

The hot-film systems were tested in the configuration to be used in the field with 12 v tractor batteries supplying power to the probes, and initially at the field overheat temperatures. Later tests were made at a variety of overheat temperatures. With the no-flow output voltage suppressed and the linearizer controls adjusted as they would be in the field, repeatable curves such as those shown in Fig. 14 were obtained for each system. Deviations from linearity were at most 3% of the indicated flow at any point on the curve. These curves seemed to be independent of the operating temperature of the probe for any given system, a desirable feature but one which required explanation.

The explanation was discovered during an investigation of another aspect of the calibration of the system. If the zero suppression was not done precisely, the slope and

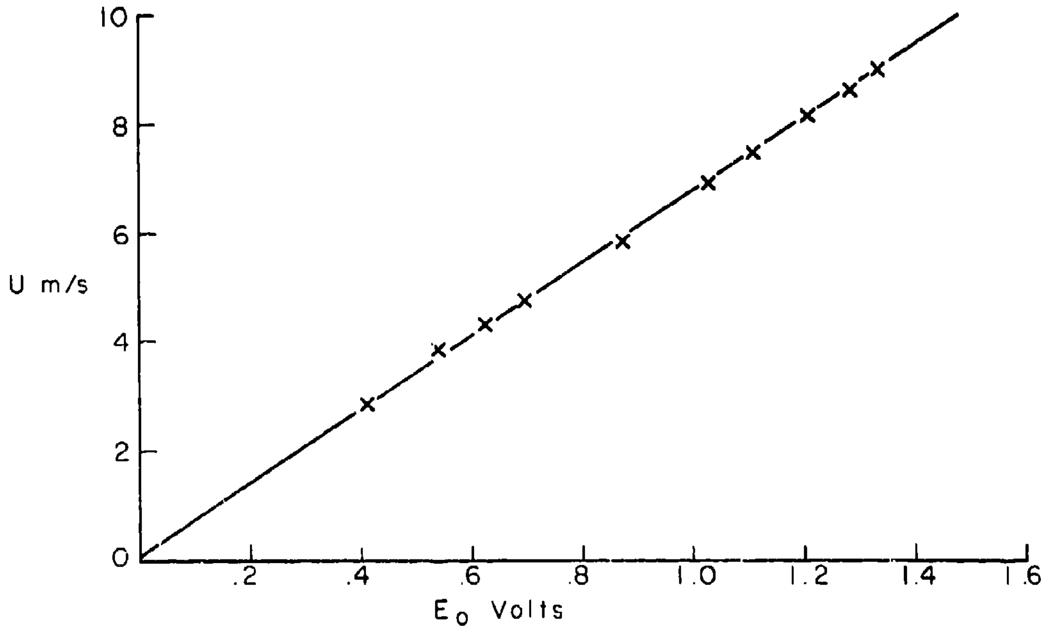

Fig. 14. Hot-film calibration curve for zero suppressed system

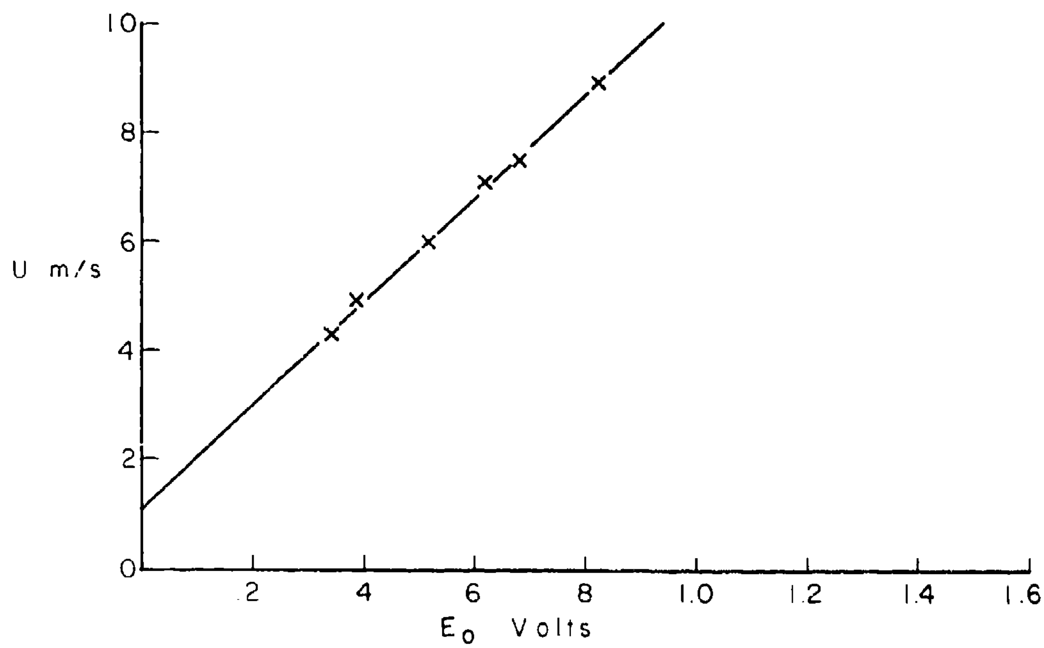

Fig. 15. Hot-film calibration curve for unzeroed system

intercept of the curve changed, Fig. 15. The change in intercept was to be expected. The change in slope was an unpleasant surprise which indicated that the gain of the system was a function of the zero suppress control position.

The instruction manual for the 55D15 linearizer gave no indication that the gain would be a function of the zero suppression control position. Therefore, I decided to check the units against the diagram in the manual. They agreed. I then derived the transfer characteristics of the unit from the circuit diagram. The result explained what I had observed. The actual transfer function for the 55D15 is

$$E_{out} = \left[C\ (KE_{in} - V_o)\right]^m \text{ where}$$

K is a constant determined by the zero suppress control,

V_o is a constant determined by the min/max% control,

C is a constant determined by the gain control, and

m is a constant determined by the exponent control.

The derivations of this expression and the conclusions following are contained in a College of Marine Studies Technical Report, The University of Delaware, presently in press. Because copyrighted material is involved it will not be reproduced here. If one substitutes King's Law in the form

$$E_{anem} = \left[(1 + \frac{B}{A} U^N) \, A \, \Delta T \right]^{1/2}$$ into the transfer function for the linearizer, one gets

$$E_{out} = (CV_o)^m \left[(1 + \frac{B}{A} U^N)^{1/2} - 1 \right]^m$$ for a properly zeroed system. Thus the gain for a zeroed system is independent of both the overheat temperature ΔT and of the position of the zero-suppress control so long as the system is balanced.

For a given overheat, the gain is clearly a function of K under unbalanced conditions. But the function is now known. Thus a correction can be applied to date taken while the control is misset if the resulting offset is not too large, Merceret (in press). The correction consists of a shift and a scaling, thus

$$E_{corrected} = \frac{1}{G} (E_{out} - E_o) \quad \text{where}$$

E_o is the shift voltage equal to $E_{out}(U = 0)$ and G is the gain of the system relative to the gain of a properly suppressed system, which function may be determined by computation or by measurement for each unit as a function of the value of E_o. Because we had recorded E_o in the field we were able to correct for the error in those runs for which E_o was not exactly zero. Details of the method are presented in the afore mentioned

CMS Technical Report. Of the eleven reels of data we collected, six required no correction, three were corrected, and two were discarded as being beyond the range for which reliable corrections could be made.

The final step in the laboratory checkout of the instrumentation was to calibrate the film systems and cup anemometers against each other over the speed range of 1 - 10 m/s. The systems agreed within ±2% of the indicated velocity.

We also tested the tape recorder in the laboratory After an initial problem was solved which required returning the unit to the factory for repair, the machine performed within specifications under test. Nonetheless, in case the recorder was adversely affected by the temperature or voltage fluctuations likely in the field, we took the precaution of placing record system calibration marks on the tape. A switch-box containing the voltage divider permitted each channel to be selectively connected to a 3.1 v reference source or effectively grounded by the divider network before signals were applied, see Fig. 16. If the carrier frequency or gain of the recording system varied, it would show up as a zero or reference voltage shift respectively at playback, and a suitable correction could be applied to the data. In no case on the field tapes did such a shift actually occur.

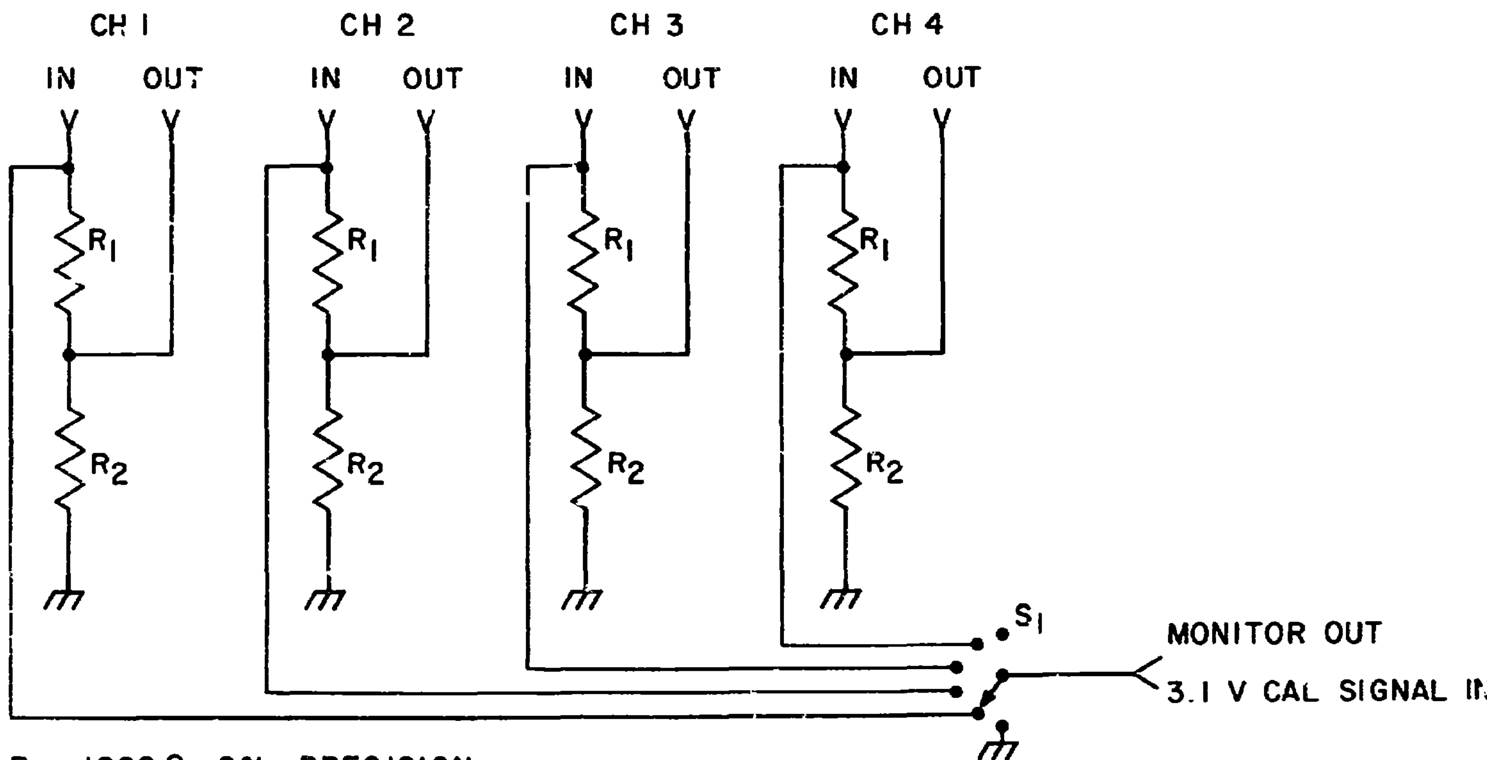

$R_1 = 1000\,\Omega$ 2% PRECISION
$R_2 = 510\,\Omega$ 2% PRECISION

Fig. 16. Circuit diagram of tape marker and signal divider

VI. THE RECOVERING AND THE PROCESSING OF THE DATA

The thermometric data and those from the cup anemometers were in numerical form as taken and could be plotted or fitted to profiles numerically without processing except for converting cup counts to velocities by a simple multiplication in each case.

The data from the hot-film systems were recorded on tape as analog signals convertible to voltage linearly proportional to sensed wind speed as a continuous function of time. The constant of proportionality for each system was determined from the calibration curves. It was necessary, therefore, to process the electrical signal to determine the mean voltage for each run to obtain profile values, and to look at the energy contained in the signal above 20 Hz to examine the burst structure. While we had originally intended to use electronic analog processing to obtain the information we required and to produce turbulent one-dimensional energy spectra as well to determine as much as possible about the structure of the flow, we were unable to carry out these plans for financial reasons. Moreover we found that the rented recorder had to be returned within two weeks of the completion of the field work. Thus we would lose our playback facilities.

To avoid the unpleasantness of having reels of valuable but inaccessible data we devised another method of processing the information which would give us all that we needed and most of what we wanted except spectra. We placed a rush order for two Heathkit Model EU20B chart recorders with variable speed drives, manufacturer's specifications for which are presented in Tables 6 and 7. The data would be transferred from magnetic tape to charts using the fastest available chart speed of 5 sec/inch, the low frequency signal components on one chart and the high frequency components on the other. The separation used a low pass filter and a high pass filter with their inputs in parallel, their outputs being routed to the low frequency information storing recorder and a rectifier-filter system respectively. The output of the rectifier-filter system went to the high frequency information storing recorder. A circuit diagram of the system is shown in Fig. 17. The high pass filter was a General Radio Model 1952 Universal Filter operated in the high pass mode with a cutoff frequency setting of 20 Hz. Manufacturer's specifications and rejection curves are shown in Table 8 and Fig. 18, respectively. The low pass filters between the tape and the low frequency chart recorder, and between the rectifiers and the high frequency chart recorder were designed to severely attenuate signals above 10 Hz to avoid causing any instabilities in the chart recorders. The chart recorders have 60 Hz choppers in the servo-system and the system can begin to "hunt" wildly if

CHART PAPER: grid width: 10 inches; length: 120 foot roll; markings: 0 - 100

CHART SPAN: five fixed ranges: 10, 25, 50, 100, and 250 mV; plus a vernier adjustment between each fixed range, which provides adjustment of span to any value between 250 and 3.3 mV. There is also an external position for special plug-in fixed ranges

BALANCING TIME: 0.1 second per inch, 1 second full scale (10 inches)

INPUT CIRCUIT: self-balancing potentiometric on all ranges

INPUT RESISTANCE: essentially infinite at null. Approximately 500 kΩ off null

LINE FREQUENCY REJECTION: 80 db in common mode

FLOATING INPUT: 100 v DC maximum above ground. 70 VAC rms maximum across the negative input terminal and GND terminal

OVERALL ERROR: less than 1% of full scale from 10 to 250 mV

DEAD ZONE: less than 0.5% of full scale from 10 to 250 mV

LINEARITY: less than 0.5% full scale

MAXIMUM RECOMMENDED SOURCE RESISTANCE: 50 kΩ

REFERENCE SOURCE: zener regulated supply

POWER REQUIREMENTS: 120 volts, 60 Hz; 45 watts

DIMENSIONS: 14"W × 8-3/4"H × 13-1/4"D

Table 6. Manufacturer's specifications for chart recorder supplied by Heath Company

CHART SPEEDS:

5 seconds to 2 hours per inch in 21 speeds when using the internal chart drive signal. Any chart speed up to 5 seconds per inch when using an external chart drive signal

CHART ADVANCEMENT STEPS:

600 steps per inch; 2 steps per cycle of the signal applied to the motor drive circuit. The motor will accurately step from 0 to 40 cps and will run accurately at 60 cps

TRANSISTOR COMPLEMENT:

27 - 2N3393: Schmitt trigger, binaries, and emitter follower. 2 - 2N3416: motor drive

DIODE COMPLEMENT:

29 - 1N191 crystal diode: twenty-four binary and five feedback diodes. 1 - 1N751 zener diode: D.C. level adjuster 2 - 750 mA 100 v PIV silicon diodes: supply rectifiers

CONTROLS:

21-position chart speed switch. External-internal signal switch

POWER REQUIREMENTS:

105-125 volts AC, 60 cps, 30 watts

Table 7. Manufacturer's specifications for chart drive supplied by Heath Company

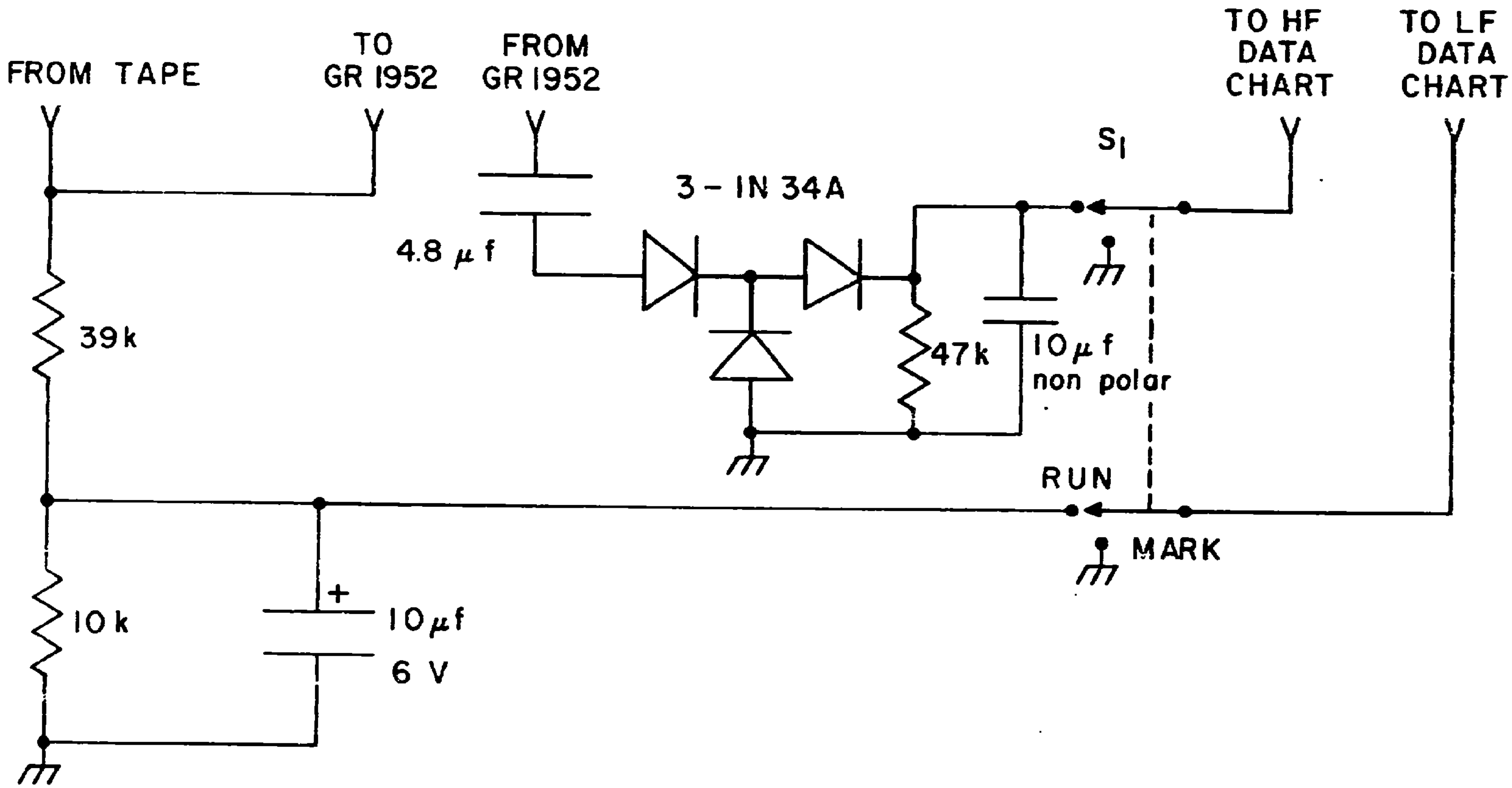

Fig. 17. Tape to chart signal conversion circuit

FREQUENCY RANGE

CUT-OFF FREQUENCIES: adjustable 4 Hz to 60 kHz in four ranges

PASS-BAND LIMITS: low-frequency response to D.C. (approximately 0.7 Hz with A.C. input coupling) in LOW PASS and BAND REJECT modes. High-frequency response uniform ±0.5 db to 300 kHz in HIGH PASS and BAND REJECT modes

CONTROLS: log frequency-dial calibration; accuracy ±2% of cut-off frequency (at 3-db points)

FILTERS

FILTER CHARACTERISTICS: filters are fourth-order (four-pole) Chebyshev approximations to ideal magnitude response. The nominal pass-band ripple is ±0.1 db (±0.2 db max); nominal attenuation at the calibrated cut-off frequency is 3 db; initial attenuation rate is 30 db per octave. Attenuation at twice or at one-half the selected frequency as applicable, is at least 30 db

TUNING MODES: switch selected, LOW PASS, HIGH PASS, BAND PASS, and BAND REJECT

INPUT

GAIN: 0 or -20 db, switch selected. Accuracy of gain is ±1 db, of 20 db attenuator is ±0.2 db

IMPEDANCE: 100 kΩ

COUPLING: A.C. or D.C.. Lower cut-off frequency (3 db down) for A.C. coupling is about 0.7 Hz

Table 8. Manufacturer's specifications for bandpass filter supplied by General Radio (continued on page 52)

Table 8. continued from page 51

GENERAL

OUTPUT: 600 Ω impedance

NOISE: 100 μV in an effective bandwidth of 50 kHz

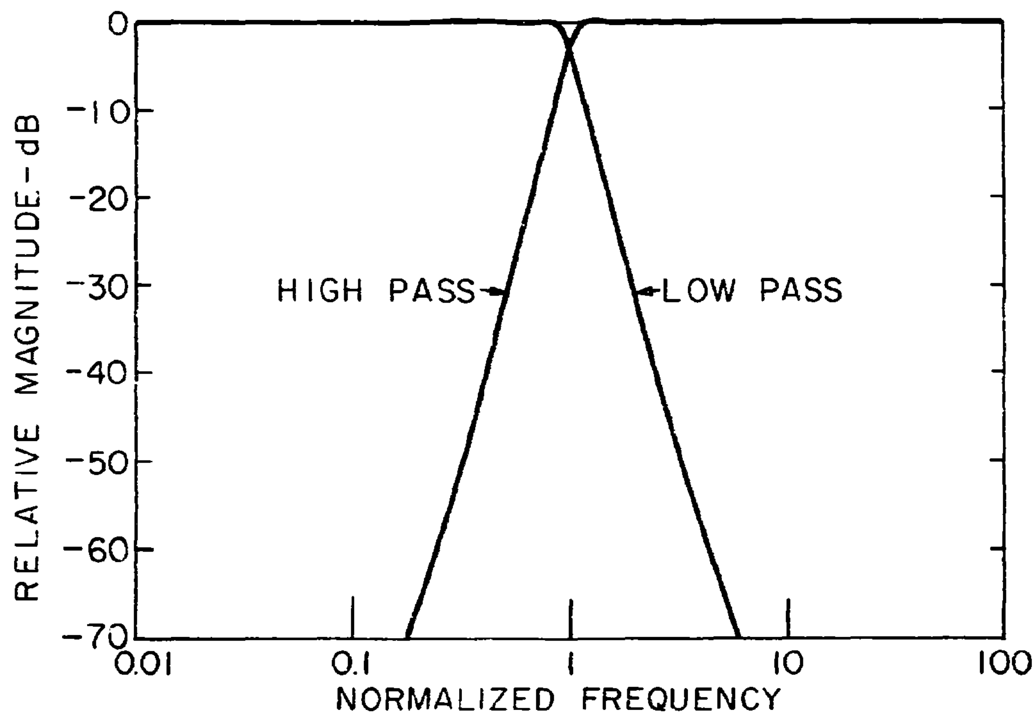

Fig. 18. Frequency response of GR model 1952 filter supplied by General Radio

60 Hz energy reaches the amplifiers. This filtering also smoothed the record somewhat and made it easier to read without removing much of the detail. The chart pens would each respond substantially to changes with time scales longer than 200 ms. At time scales of 800 ms or larger essentially complete response was obtained.

A provision to place simultaneous marks on the high and low frequency charts allowed for the possibility of synchronizing the charts even if the chart speeds differed slightly. The precaution proved to be unnecessary, the recorders always agreeing within 2 seconds after a 30 min run, and within one second from any intermediate mark to the closer end of the chart where signal marks denoted the beginning and end of each tape. Since the minimum practically resolvable time difference between events on the charts was about 1 second this meant the chart synchronization was for practical purposes perfect.

We could now use graphical averaging techniques on our paper chart record. We had replaced the expense of electronic analysis with the labor of manual date reduction.

The pairs of charts--one high frequency information chart and one low-frequency information chart per channel from the tape--were filed according to data and run number and marked with information about the system and height from which its record came. Because we would sample the mean velocity selectively if bursts were occurring in the high frequency energy, the high frequency charts of each run were analyzed first. It is necessary here to preview the results in order to explain subsequent processing of the data. Bursts were observed at all levels simultaneously in each run in nearly every case where a burst was seen in any record. Figure 19 shows a typical burst, while Fig. 20 shows bursts occurring simultaneously at each height with the charts time synchronized using the calibration and end of record marks.

Each set of high frequency charts containing records from three heights during a given run was time synchronized using the spikes at the beginning and end of recording, see Fig. 21, and examined for bursts. Judgements were made as to where bursts appeared in each set of records and the regions of burst activity marked on each chart, see Fig. 22. These marks were transferred to the low frequency records after they had been time-mark synchronized with the high frequency graphs. Thus the mean velocity record could be selectively sampled.

The bursts were sufficiently marked that when I asked visitors to my office to pick them out, they repeatedly identified them and marked the leading and trailing edges within a second or two of my judgement; thus the method was a consistent and simple one to use. Any algorithmic system

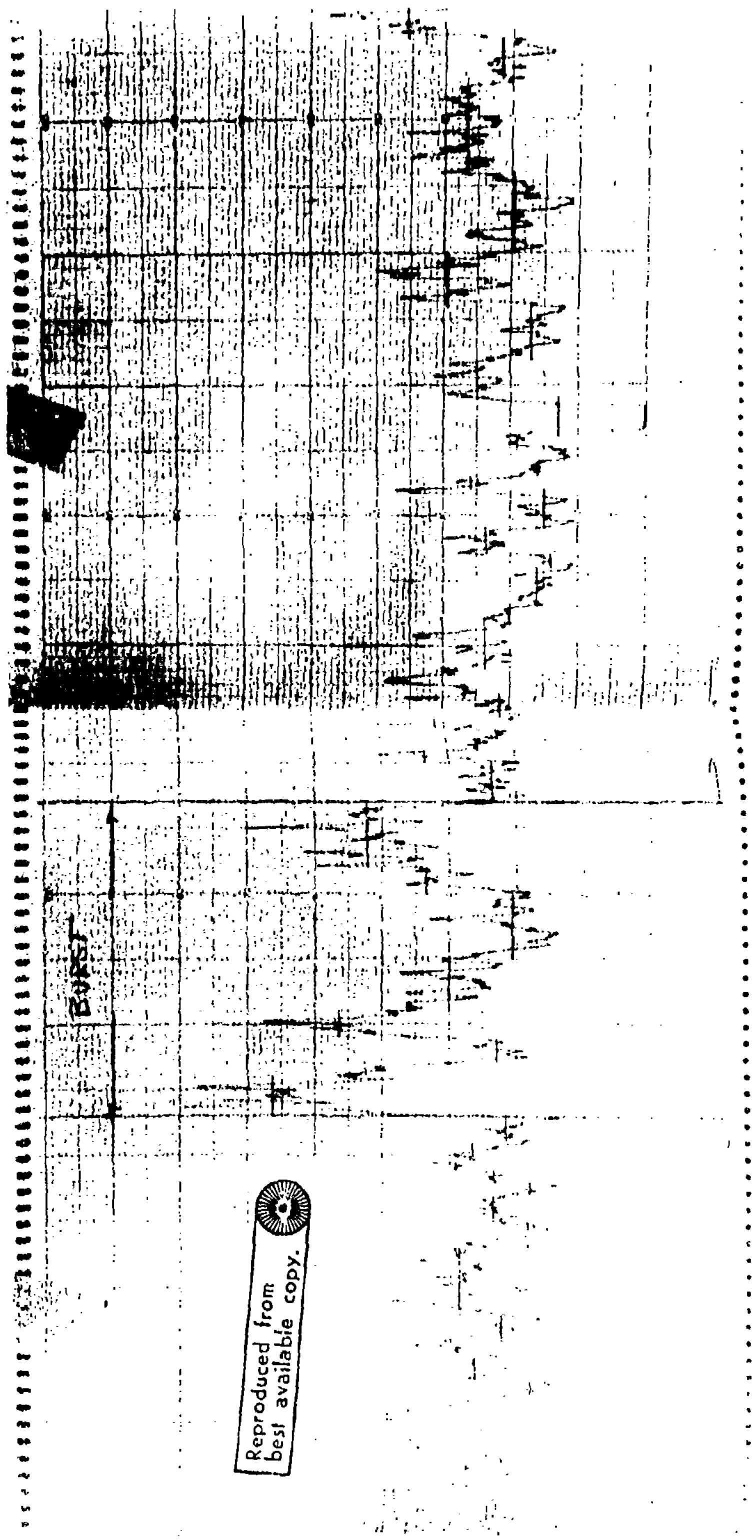
BURST

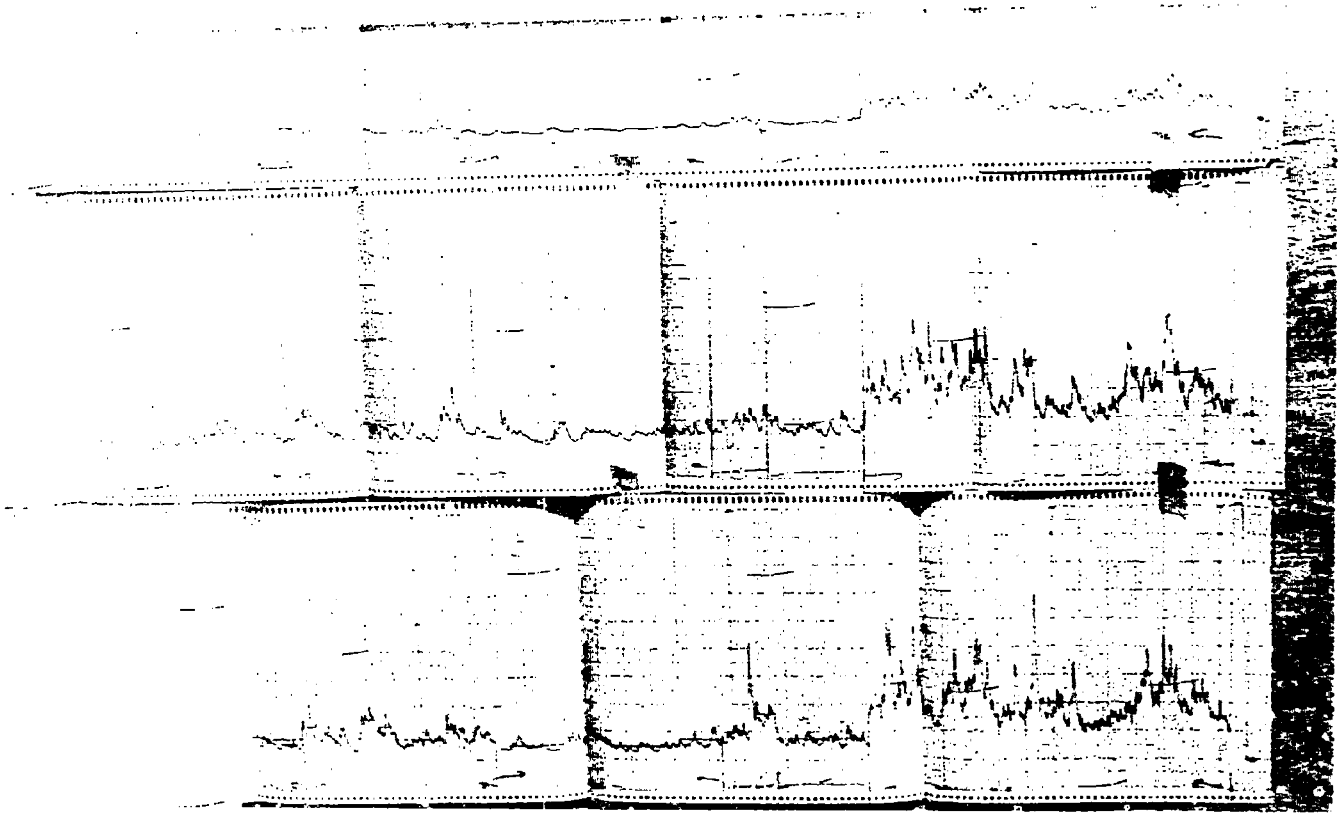

[illegible] time synchronized records

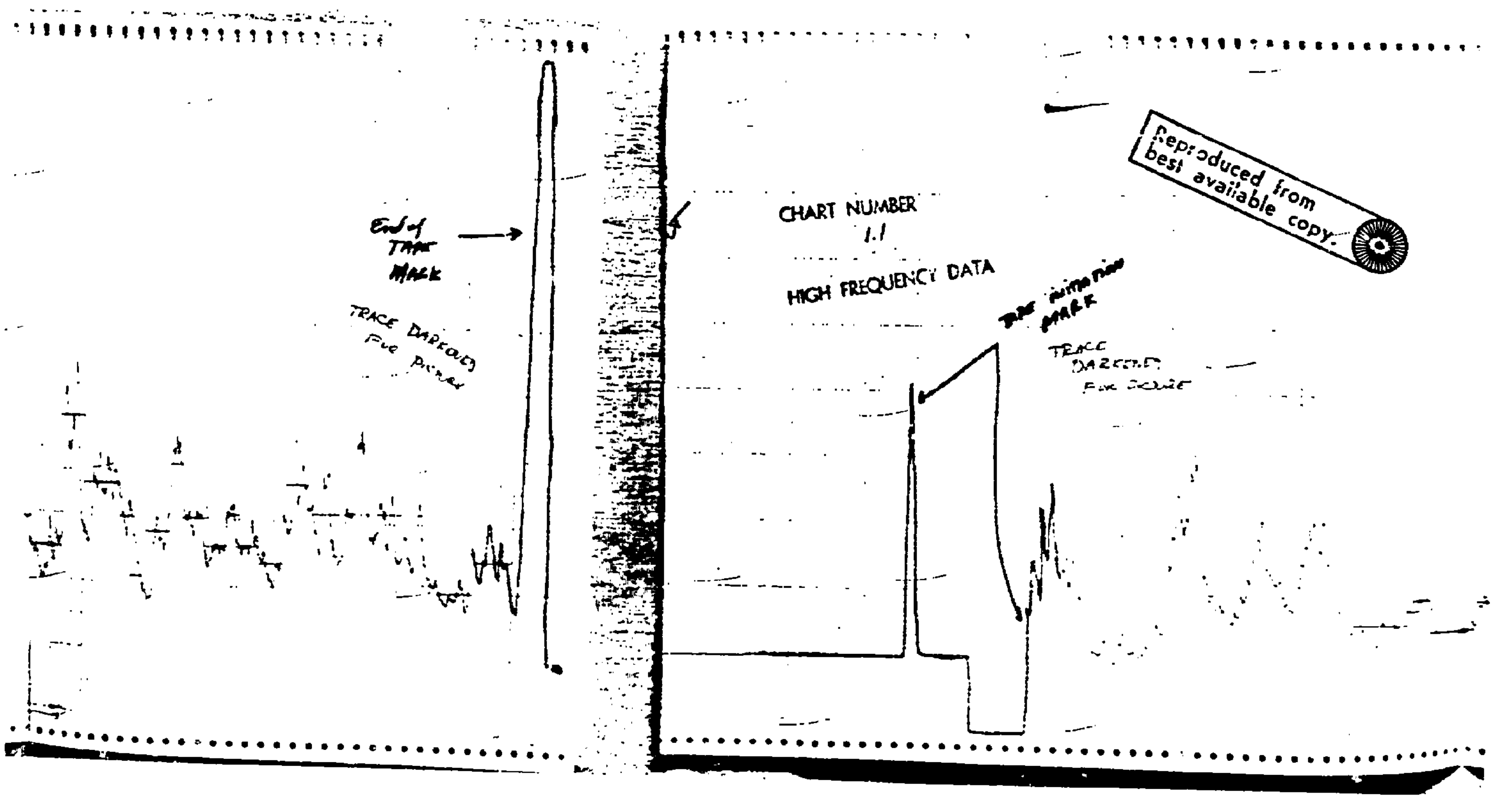

Fig. 21. Marks used for time synchronization of various levels

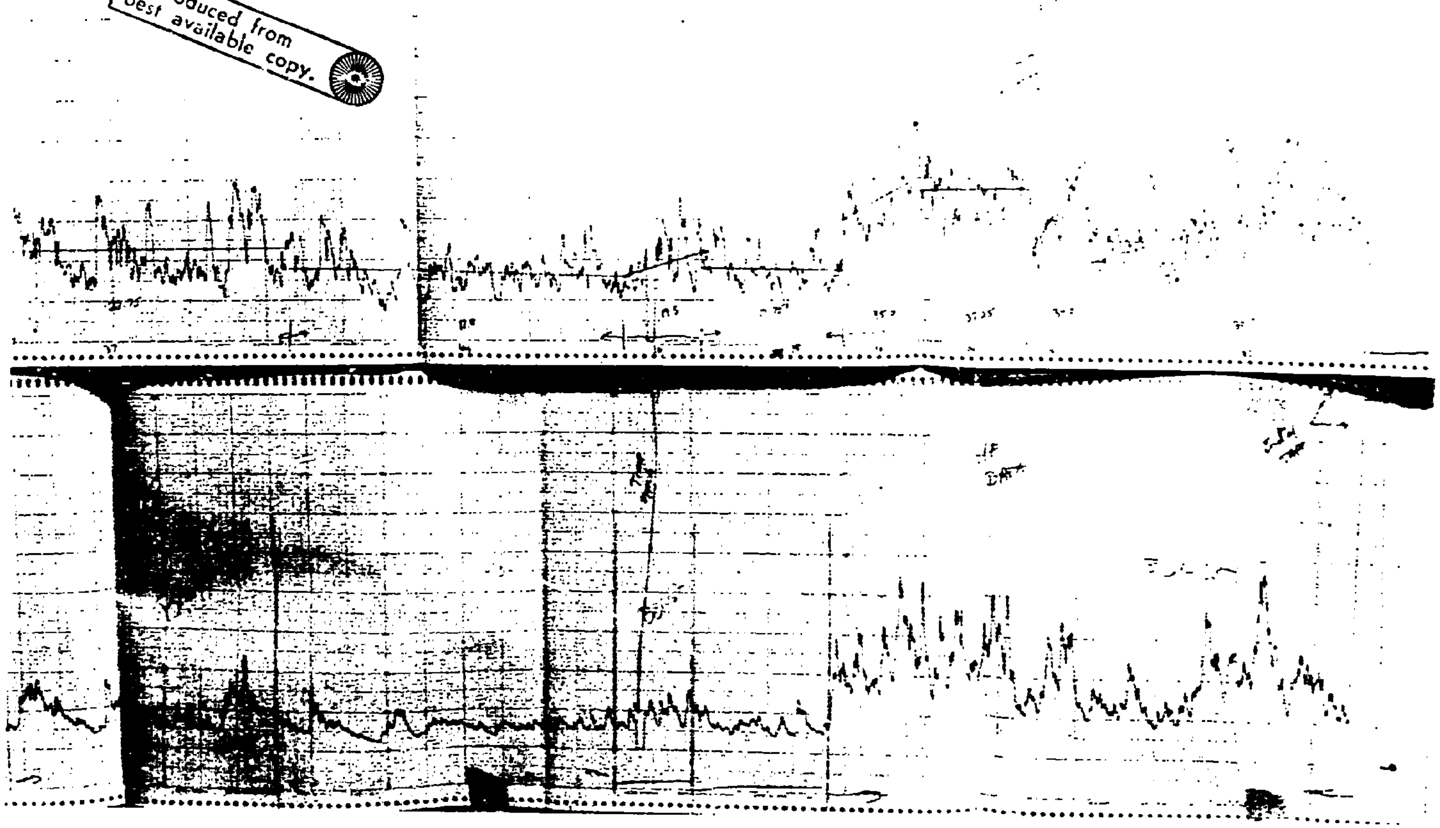

Fig. 22. Burst region marks transferred from high frequency to low frequency records

such as marking a burst whenever the trace exceeded a certain level involves decisions as to where to place the marker level and thus the human judgement is not removed, it's just better concealed. Moreover, there were trends in the data which would cause difficulty in consistently applying any algorithm to select bursts. Since we were looking for a structure of a particular and readily distinguishable kind superimposed on trends of other kinds, the trained human intellect seemed the tool most likely to produce meaningful results.

Having selected which parts of each record were to be averaged together it was necessary to choose a procedure for averaging the data from the charts. The first method we considered was the use of a planimeter to integrate the trace but repeated trials showed variations of as much as 5% in the value obtained. We decided to see what happened if we just "eye-balled" a straight line through short sections of the graph and computed average values from the line segments. The results were pleasantly surprising: the answers were always within ±2% of the mean of the planimeter readings and the technique was much quicker. The average for each segment was taken to be the value at center of the straight line defining the segment and the length of the segment was used as a weighting factor in computing the overall average on a Wang Model 500 calculator. The accuracy of the method is confirmed by the results of the instrument checkout run, which are reported in Chapter VII.

In addition to the mean velocity information we desired a measure of the energy above 20 Hz within and without the bursts. Because we could not calibrate the detector network and filter system for the unknown spectral shape of the incoming signal, lacking the necessary equipment, the measure would have to be a relative one and would be that only if the spectra above 20 Hz maintained approximately the same shape regardless of amplitude. In the inertial subrange this would be the case.

If the utility of the relative measure be granted, obtaining a mean square still is somewhat more difficult than obtaining a mean. As with the means, I examined mechanical methods of integrating the squares of the values of the curves and tested various graphical techniques. I came to the conclusion that short horizontal line segments, much shorter than those used for mean values, should be employed and their position squared and averaged with the appropriate weighting. If the value of the line in any segment was ξ, and the graph's fluctuations from that value within the segment ξ', then

$$\overline{\hat{\xi}^2} = \overline{\xi^2} + \overline{\xi'^2}$$

where $\overline{\hat{\xi}^2}$ is the true mean square value of the graph in the segment. Since ξ is a constant, $\overline{\xi^2} = \bar{\xi}^2$ and thus, if the segment is made small enough that $\overline{\xi'^2} \ll \bar{\xi}^2$, then $\overline{\hat{\xi}^2} \approx \bar{\xi}^2$. The segments were picked accordingly.

The Wang Model 500, a programmable desk computer-calculator, was used for the arithmetical analysis of the data. When geometrical averages were wanted, a program for arithmetical averages was used entering the logarithm of each datum. The antilogarithm of this mean is the geometric mean. Applying "exponentiation" to the standard deviation of the mean of the logarithms yields a value which pertains to the deviation in ratio rather than the deviation in value from the mean.

Because the directional responses of cup anemometers and hot-film anemometers are quite different, a directionally varying wind could cause the two kinds of instruments to give different results for the mean wind at a given height and thus "warp" the profile. Our method of dealing with this possibility, for the lack of anything better, is as follows. If we assume the wind vectors are parallel at all heights sensed by our instruments then the ratio of

$$\frac{U(\text{measured cup})}{U(\text{measured film})} \text{ will be the same for any height.}$$

It will be greater than one since the hot-films respond less than fully to winds at an angle to their direction of maximum sensitivity (for which the calibrations apply) while the cups are omni-directional in the horizontal. Since we had a cup and a film together at one height we computed the ratio and multiplied it into the velocities obtained from the lower films and based the results on cup-equivalent velocities. The distribution of values obtained is displayed in Table 9. Their relative reliability was considered in reviewing the data but the profiles did not seem to be poorer when larger factors were involved.

No. of Acceptable Runs	7	3	3	4	1	2	1	0	0	1
Wind Factor	1.00	1.05	1.10	1.15	1.20	1.25	1.30	1.35	1.40	1.45

Table 9. Distribution of wind factors

VII. THE RESULTS

One of my immediate concerns following the completion of the field work was for the accuracy and precision which I could expect after the whole process of reducing the data had been completed. The errors of analysis usually compound the errors of measurement and recording. How good would the final result be?

Before we began profile measurements we made three checkout runs with the hot-films mounted side by side with a cup anemometer as a reference at 90 cm during winds typical of those encountered during the profile measurements. The results indicate we may have considerable confidence in the overall system. In Table 10 are displayed the ratios of the mean velocity values obtained from the graphic averaging procedure for hot-film systems A, B, and C to that obtained from the reference cup anemometer in each run. Of the nine entries, five show an overall error smaller than or equal to 3%, and only one exceeds 7%. These data were taken during intermittent snow showers and sunlight which presented the worst operating environment in which we had to work and with the instruments over different parts of the furrows, thus inducing a small systematic error in the data. Together with the high values obtained for the correlations to logarithmic profiles, these data indicate an overall system accuracy of considerably

Run	Cup Velocity Average (m/s)	A/Cup	B/Cup	C/Cup
1	7.42	1.06	0.97	1.02
2	5.85	1.03	0.93	1.01
3	7.30	1.07	0.99	1.08

Table 10. Ratios of hot-film mean velocities to reference cup mean velocities

better than 10% in each case and better than 5% in perhaps half of the data.

My next concern was to examine the charts to determine whether or not bursts were present, and whether they appeared randomly, sequentially, or simultaneously at the various levels. Once I knew the nature of the phenomenon I could begin computing averages and profile parameters.

The purity of the results was unexpected. Each of the three high frequency records from the 22 acceptable runs was searched and marked for bursts. In no run were there any bursts which did not occur simultaneously (±1 second at the leading and trailing edges) at all three levels! This may well mean that there is an unexpectedly rapid exchange of turbulent properties in the flow. This will be discussed in subsequent paragraphs. The intermittency factor, I, defined as the ratio of time occupied by bursts to the length of the record, ranged from 0.27 to 0.82 in an irregular way. Table 11 shows the distribution of values. Clearly, most of them fall between 0.50 and 0.69. Thus it might have been more orthodox to have defined the regions of lower level activity as "bursts" since they comprise the smaller part of the records.

The time between bursts and burst length seemed to exhibit no detectable pattern even though other experimenters

Range	Number of Runs having I within the Range
0.20 - 0.29	2
0.30 - 0.39	1
0.40 - 0.49	1
0.50 - 0.59	6
0.60 - 0.69	8
0.70 - 0.79	3
0.80 - 0.89	1

Table 11. Distribution of intermittency values

have noted that the burst rate in laboratory work correlates somewhat with friction velocity, Kim, Kline, and Reynolds (1971), at smaller friction velocities than occurred in our work. Typical bursts lasted from 5 to 50 seconds with modal values around 15 seconds. The intervals between bursts were similar. We did no detailed analysis on the burst frequencies and lengths after determining that no significant correlation with other variables was to be found.

There were 88 profiles resulting from the 22 runs. Mean velocities were computed from the hot-film systems for the portions of the records within bursts, without bursts, and both combined. Additionally, this last was also computed with the cup anemometer data included. The data were fitted to

$$z = z_o \, e^{kU/u*} .$$

The correlation coefficients were quite high. Table 12 shows their distribution.

The major factor contributing to a poor correlation coefficient at the lower levels in some runs was the effect of lapse rate on the profile. In all but four of the 33 cases where the correlation coefficient was smaller than 0.98 the lapse rate in the lowest meter was greater in magnitude than 0.5 C per meter and negative thus indicating

Range of Corr Coeff*	Cups & Films Total Record	Films Whole Record	Films Bursts	Films Bursts Elim	TOTAL
0.98-1.00	22	10	11	12	55
0.96-0.98	0	6	2	5	13
0.94-0.96	0	4	6	1	11
0.92-0.94	0	1	2	2	5
0.90-0.92	0	1	1	1	3
0.88-0.90	0	0	0	0	0
0.86-0.88	0	0	0	0	0
0.84-0.86	0	0	0	0	0
0.82-0.84	0	0	0	1	1
TOTAL	22	22	22	22	88

* Class intervals are open to the right

Table 12. Distribution of correlation coefficients

that strongly unstable conditions obtained. On the other hand, only four correlations less than 0.98 occurred with lapse rates closer to neutral than -0.5 C/m.

The lack of large variation between the goodness of fit to the logarithmic formula among the three kinds of profiles made with the films may indicate that the adjustment of the profile to new conditions is quite rapid. This is further supported by some tests conducted low over the furrows. The test was intended to examine the structure of the flow over the furrows by measuring profiles as a function of phase with respect to the furrows. This was not done because the cup anemometers were not available on the day allotted to the experiment, but hot-film data were obtained along a line normal to the crest lines 10 cm above the top of the crests, see Fig. 23. The results showed that the velocity at 10 cm (1/9 wavelength, 1 peak to peak amplitude) above the furrows was, within ±15%, the same as if a logarithmic profile having the same roughness length as obtained for our other records had been mechanically lifted without change in shape to follow the contour of the furrow. For a 1 m/s wind at probe height the time to pass the 22 cm between probes is about 200 ms. The data are inadequate to determine whether the quick adjustment to the change in position of the surface attenuates with height. The conventional wisdom is that rapid attenuation should occur but the simultaneity of the appearance of

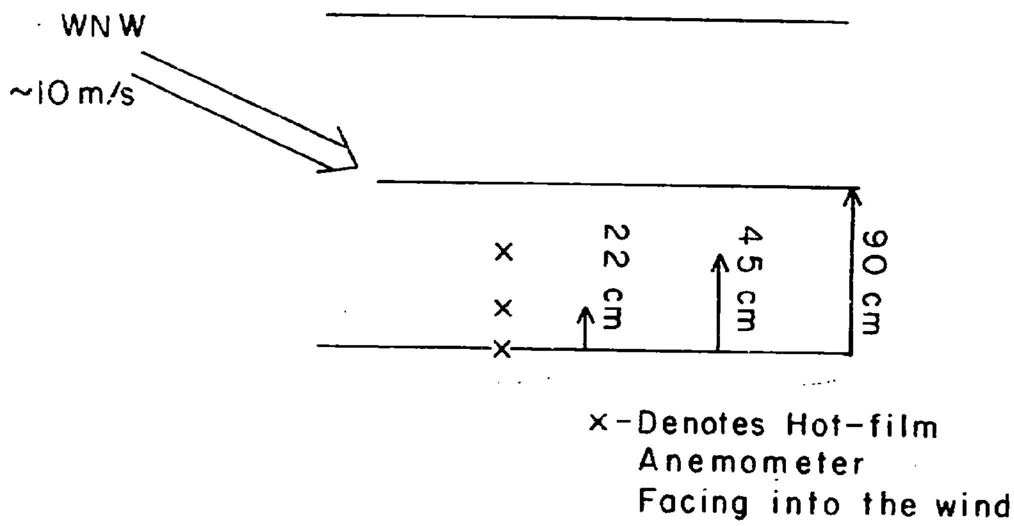

Fig. 23. Geometry of the furrow phase effect experiment

bursts implies so high a rate of vertical transport of flow properties that the attenuation may not occur. The adjustment of the profile may explain why Takeda (1963) had difficulty following the evolution of wave induced kinks in profiles passing over sand bars, the kinks disappearing so swiftly that they were undetectable by the time they reached his land stations.

Since the bursts occurred simultaneously at all levels and since the profiles adjusted rapidly enough that good correlations were obtained within and without the bursts, our data were appropriate for examining the parameters of the logarithmic profiles to test Ruggles' hypothesis.

Before I began the search for systematic variations of z_o and u* as a function of U_{10} and the bursts, I marked the 22 runs with "flags" indicating in each of the 4 profiles of each run such anomalies as one would not expect to find in "perfect" data. Flags were given for the following reasons:

Lapse rate steeper than	-0.5 C/m
Correlation	<0.98
$\dfrac{u^* \text{ (burst)}}{u^* \text{ (3 level combined)}}$	<1.0
$\dfrac{u^* \text{ (burst absent)}}{u^* \text{ (3 level combined)}}$	>1.0
$\dfrac{z_o \text{ (6 level combined)}}{z_o \text{ (3 level combined)}}$	>2.0 or <0.5

$$\frac{U_{10}\ (\text{6 level combined})}{U_{10}\ (\text{3 level combined})} \quad >1.1 \text{ or } <0.9$$

$$\frac{U_{10}\ (\text{burst absent})}{U_{10}\ (\text{3 level combined})} \quad >1.0$$

$$\frac{U_{10}\ (\text{burst})}{U_{10}\ (\text{3 level combined})} \quad <1.0 \quad .$$

The largest number of flags which could be placed on any single run was eleven, since a correlation flag was given if one profile was insufficiently correlated, two if two, et cetera. The runs were then classified in order of reliability by the number of flags they were assigned, Table 13. The data were analyzed using the best 9, best 12, best 17, and the entire set of 22.

Because we wanted to plot z_o as a function of U_{10}, the mean wind at 10 meters, as Ruggles did, and because we had no anemometer so high, we computed U_{10} from the profile parameters of the profile for which U_{10} was desired. The result for all 88 profiles is shown in Fig. 24. Except for a hint of a slight increase in z_o near U_{10} = 6.5 m/s which may, if real, be due to some sort of instability, the roughness length, z_o, seemed relatively insensitive to everything. For each run I computed the ratios

Number of Flags N	≤2	3	4	≥5
Number of Runs having N Flags	9	3	5	5
Number of Runs having N or Fewer Flags	9	12	17	22

Table 13. Distribution of flags

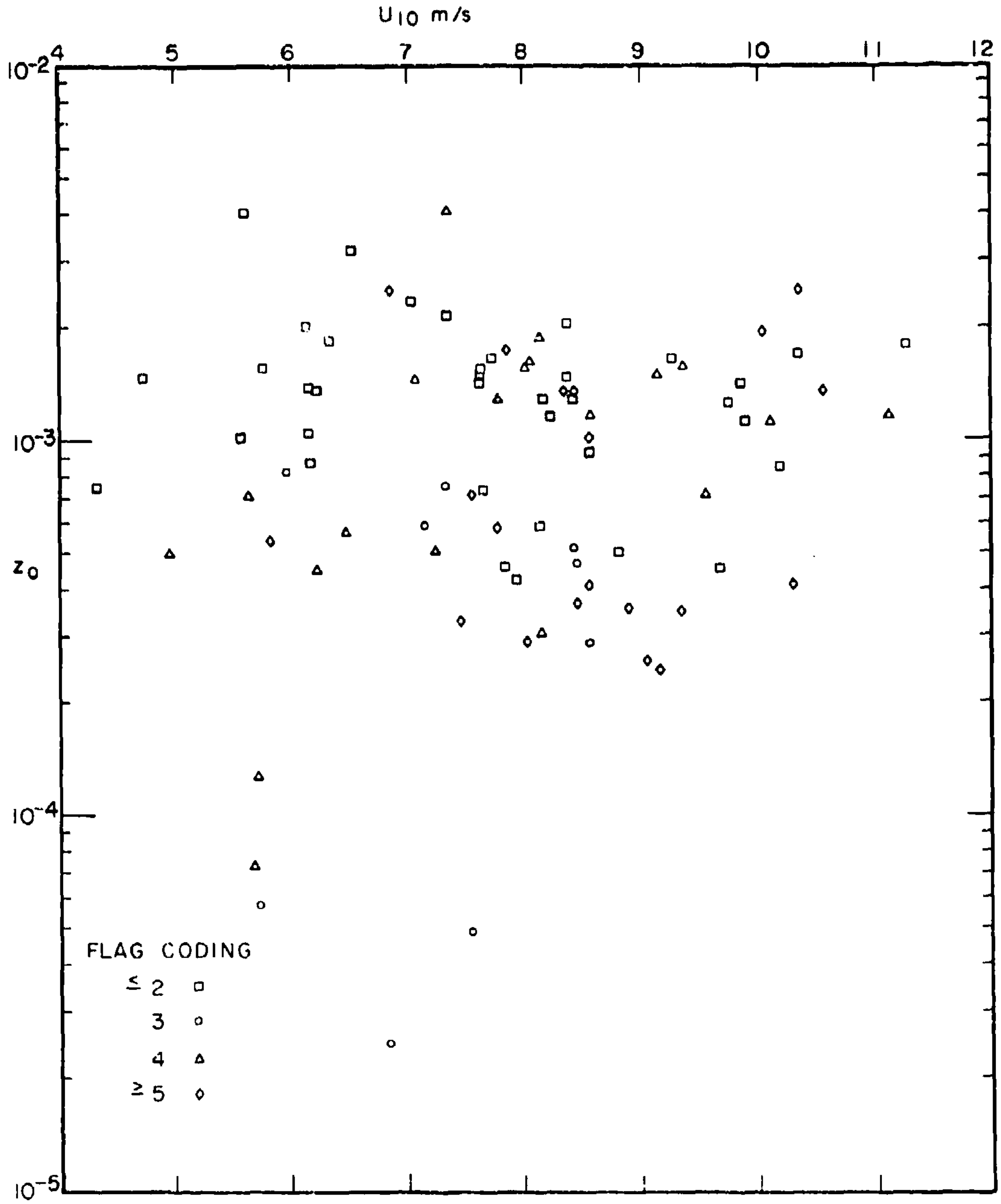

Fig. 24. z_o *vs.* U_{10}

$$\frac{z_o \text{ (burst)}}{z_o \text{ (3 level combined)}} \quad \text{and} \quad \frac{z_o \text{ (burst absent)}}{z_o \text{ (3 level combined)}}$$

and calculated their geometric and arithmetic means and standard deviations, Table 14. The mean values of the ratios are close to unity within the precision of the system. The arithmetic and geometric means and standard deviations do not differ greatly. Thus a separate computation of the geometric mean and standard deviation for z_o seems unnecessary. The arithmetic mean values and standard deviations for z_o are presented in Table 15. The only trend is a slight decrease in z_o as the quality of the data decreases. This happens to correlate with an increasingly unstable lapse rate but the magnitude of the trend and the sample size are both so small as to be insufficient for drawing any conclusions.

If the roughness length seems relatively unaffected by changes in both the mean wind and the burst structure, what about the friction velocity? Figure 25 shows u* *vs.* U_{10} for all 88 profiles. Except for a hint of scatter near 6.5 m/s, the data clump uniformly about a straight line $u^* = -0.035 + 0.0469\ U_{10}$ with a correlation of 0.895. Table 16 shows the variation of u* with the burst structure. While the magnitude of the ratios is of the same order as that for the ratios of z_o's, the value for σ is smaller. Thus, these variations

Selected Data	9 Best	12 Best	17 Best	All 22
In Bursts				
Arithmetic z_o/z_o combined	1.140	1.100	0.977	0.945
σ	0.279	0.394	0.418	0.385
Geometric z_o/z_o combined	1.096	1.021	0.858	0.896
σ	0.282	0.406	0.581	0.641
e^{σ}	1.325	1.500	1.787	1.897
Out of Bursts				
Arithmetic z_o/z_o combined	1.116	1.136	1.170	1.389
σ	0.430	0.522	0.600	0.911
Geometric z_o/z_o combined	1.030	0.981	0.987	1.132
σ	0.495	0.605	0.654	0.681
e^{σ}	1.515	1.831	1.923	1.977

Table 14. z_o ratio means and standard deviations

Selected Data	9 Best	12 Best	17 Best	All 22
Bursts				
z_o	0.00164	0.00127	0.00115	0.000989
σ	0.0014	0.0014	0.0012	0.0011
Bursts Absent				
z_o	0.00155	0.00123	0.00133	0.00129
σ	0.0011	0.0011	0.0012	0.0011
3 Level Combined				
z_o	0.00132	0.00104	0.00105	0.000937
σ	0.00077	0.00083	0.00075	0.00071

Table 15. z_o means and standard deviations

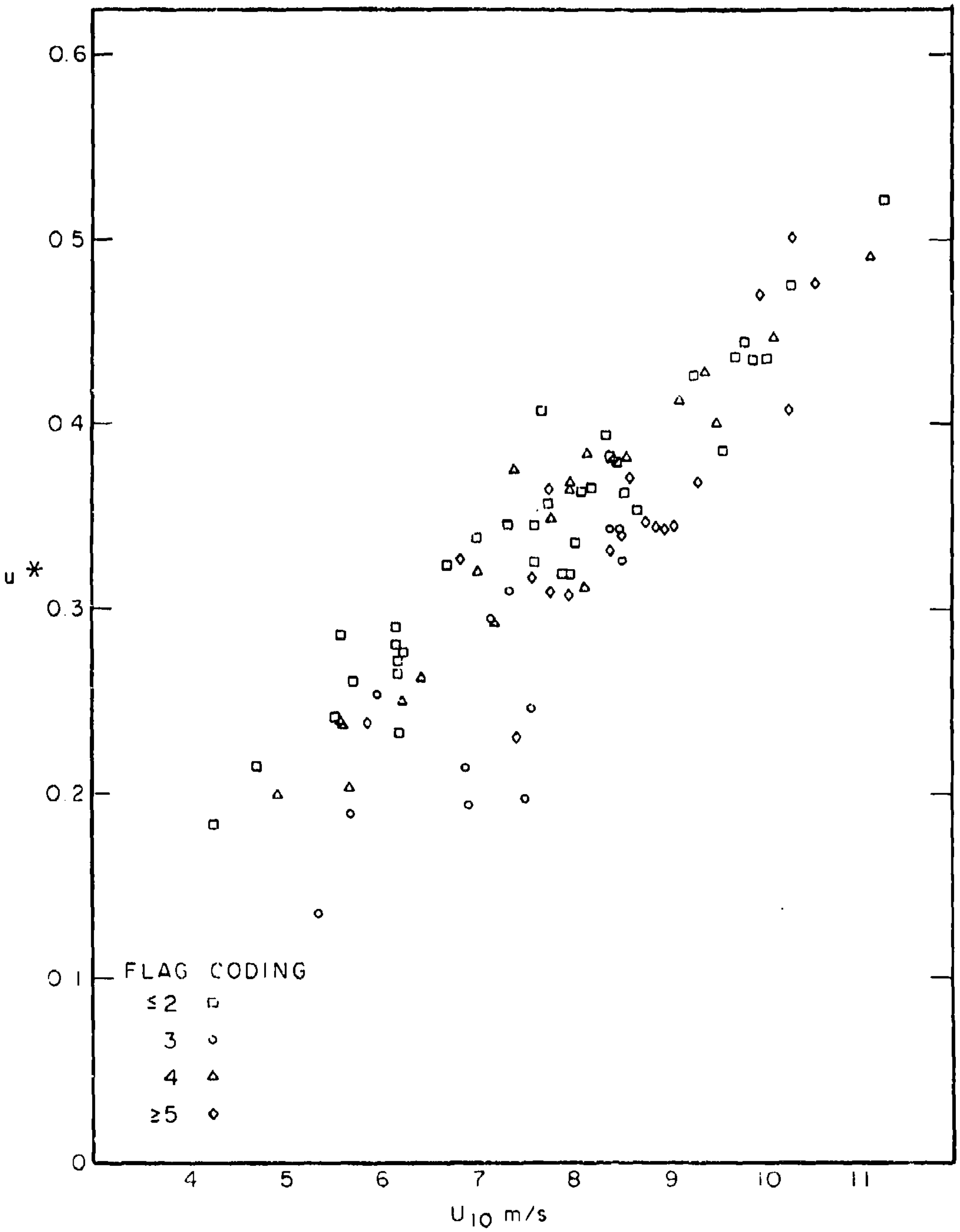

Fig. 25. u* *vs.* U_{10}

Selected Data	9 Best	12 Best	17 Best	All 22
Bursts				
u*/u* (3 level combined)	1.144	1.134	1.137	1.136
σ	0.073	0.073	0.068	0.108
Bursts Absent				
u*/u* (3 level combined)	0.835	0.830	0.865	0.885
σ	0.078	0.080	0.092	0.100

Table 16. u* ratio means and standard deviations

are more significant numerically and much more significant physically since they enter the profile linearly while the roughness length, z_o, enters the profile logarithmically.

For each hot-film profile I also computed the ratio in constant arbitrary units of u^{*2}/E_{20} where E_{20} is a quantity associated with the mean turbulent energy above 20 Hz. The averages of these values are presented in Table 17. The results indicate that the energy in the filtered portion of the turbulence above 20 Hz is an appropriate indicator but not an exact measure of the value of the friction velocity. If we use the friction velocity as the more reliable indicator of total turbulence activity in the flow, then from Table 16 we may compute the ratio

$$\left(\frac{u^* \text{ burst}}{u^* \text{ burst absent}}\right)^2 = 1.9$$

for the better data. Thus we find about twice as much turbulent energy in the bursts as outside of them. We are not sure why this seems to occur with such uniformity. Because the disparity in Reynolds numbers is so great between laboratory experiments and those in the atmosphere, laboratory experiments in intermittent flows may provide little information of use in explaining our observations.

Selected Data	9 Best	All 22
Bursts Absent		
u^{*2}/E_{20}	0.00276	0.00175
σ	0.00184	0.00161
Bursts Present		
u^{*2}/E_{20}	0.00161	0.00108
σ	0.00140	0.00105
3 Level Combined		
u^{*2}/E_{20}	0.00131	0.000861
σ	0.00109	0.000940

Table 17. Means and standard deviations of u^{*2}/E_{20}

VIII. CONCLUSIONS AND RECOMMENDATIONS

The occurrence of bursts simultaneously at all levels and the validity of the logarithmic profile within and without them indicate large vertical transport of mean momentum through the agency of nearly instantaneous adjustment of the Reynolds stresses. If the bursts were significantly swept by or frozen into the mean flow, the upper levels should see the bursts first. That they do not is a good indication that the bursts don't attach to specific fluid elements--they are purely dynamic occurrences. If this is the case, Taylor's hypothesis for converting temporal spectra to spatial spectra may be inapplicable in the lower few meters of the atmospheric boundary layer.

The lack of large peaks in the z_0 values for certain values of the wind at anemometer height, and the associated smoothness of the u^* *vs.* U_{10} curve indicate that the mechanism causing the peaks in Ruggles' data was not active in our experiment. Since, except for the rigidity of the surface, we duplicated Ruggles' work closely, it seems reasonable to conclude that the mechanism was due to the flexing of the surface. That, of course, means the mechanism was due to the presence of waves on the surface and thereby it is indicated that the waves influence not merely periodic perturbations on the profile, but the profile proper.

Since the profile is a function of the state of the sea, if waves are being generated then the profile will be changing as well and must be obtained from an adequate model as part of the solution. This complicates the already difficult problem of devising appropriate averaged field equations. The close coupling between sea and air at the interface may, however, simplify the establishment of boundary conditions.

Because the wind field contains sharply defined regions of higher turbulence activity and higher horizontal mean velocity than surrounding regions, the flow certainly can't be horizontal and two dimensional. The equation of continuity requires either significant vertical flow components or significant variability in the direction of the horizontal wind, or both, throughout the flow. Many of our simplifying assumptions for the mathematical modeling of the atmospheric boundary layer are invalid. Only a full three dimensional treatment is adequate for the micro-climatological scale analysis of geophysical flows.

The three dimensional structure may account for the arcade patterns noted on the sea surface, Kinsman (1965), page 543. The turbulent energy within the bursts is nearly twice that outside and if the remaining Reynolds stresses scale proportionately, the surface stress would be roughly doubled in the high activity regions. The result would be alternating regions of high and low wave generation activity behaving somewhat as microscale "storms" each radiating its own swell.

To make further progress in understanding the actual structure of the lower 10 meters of the atmosphere over the ocean and over land an intense investigation of the three dimensional structure of the flow should be conducted. An ideal program would involve simultaneous measurements sensing 3-component velocity profiles over heights from 3 centimeters to 10 meters at each station and taking careful records of temperature profiles as well along a line leading down-wind from land, across a beach, and out to sea with the developing wave field. The instruments should be of fast response type to allow Reynolds stresses and heat fluxes to be computed to high accuracy.

This would be expensive, but not nearly so expensive as continuing the fiction of a horizontal two dimensional flow.

BIBLIOGRAPHY

BARGER, WILLIAM R., WILLIAM D. GARRETT, ERIK MOLLO-CHRISTENSEN, and KENNETH W. RUGGLES

1970 Effects of an artificial sea slick upon the atmosphere and the ocean. J. Appl. Met. *9*(3), 396-400.

BOLE, JAMES B. and E.Y. HSU

1967 Response of gravity waves to wind excitation. Technical Report 79, Department of Civil Engineering, Stanford University.

HAUGEN, D.A., J.C. KAIMAL, and E.F. BRADLEY

1971 An experimental study of Reynolds stress and heat flux in the atmospheric surface layer. Q.J.R.M.S. *97*, 168-180.

HUSSAIN, A.K.M.F., and W.C. REYNOLDS

1970 The mechanics of a perturbation wave in turbulent shear flow. Report FM6, Thermo Sciences Division, Department of Mechanical Engineering, Stanford University.

KELLOGG, ROBERT M.

1965 Evolution of a spectrally local disturbance in a grid-generated turbulent flow. Ph.D. dissertation, Department of Mechanics, The Johns Hopkins University.

KIM, H.T., S.J. KLINE, and W.C. REYNOLDS

1971 The production of turbulence near a smooth wall in a turbulent boundary layer. J. Fluid Mech. *50*(1), 133-160.

KINSMAN, B.

1965 *Wind Waves Their Generation and Propagation on the Ocean Surface.* Prentice-Hall, 676 pp.

KRAUS, E.B.

1967 Wind stress along the sea surface. *In:* Advances in Geophysics *12*, 213-255.

LIGHTHILL, M.J.

1962 Physical interpretation of the mathematical theory of wave generation by wind. J. Fluid Mech. *14*(3), 385-398.

LUMLEY, J.L. and H.A. PANOFSKY

1964 The structure of Atmospheric Turbulence. Interscience, John Wiley & Sons, 239 pp.

MANTON, M.

1971 Mechanical Engineering Department, University of Sydney, Australia, Technical note (unpublished).

MATHER, JOHN R.

1968 meteorology and air pollution in the Delaware Valley. Publications in Climatology *XXI*(1), C.W. Thornthwaite Associates, Elmer, N.J.

MERCERET, FRANCIS J.

1968 An experimental study to determine the utility of standard commercial hot-wire and hot-film probes for measurement of turbulence in water contaminated air flows. Tech. Rept. 40, Chesapeake Bay Institute, The Johns Hopkins University, August 1968.

____

1969 An experimental study to determine the utility of standard commercial hot-wire and hot-film probes for measurement of turbulence in water contaminated air flows, Part 2. Tech. Rept. 50, Chesapeake Bay Institute, The Johns Hopkins University, February 1969.

____

1970 On the use of hot-film anemometry to measure turbulence in the presence of heavy rain. J. Appl. Met., *19*(1), 191-193, February 1970.

MILES, J.W.

1957 On the generation of surface waves by shear flows. J. Fluid Mech. *3*(2), 185-204.

____

1959 On the generation of surface waves by shear flows, Parts 2 and 3. J. Fluid Mech. *6*(4), 568-598.

____

1960 On the generation of surface waves by turbulent shear flows. J. Fluid Mech. *7*(3), 469-478.

____

1962 On the generation of surface waves by shear flows, Part 4. J. Fluid Mech. *13*(3), 433-448.

MOLLO-CHRISTENSEN, ERIK

1970 The collection of facts needed for an adequate understanding of air-sea interaction and other flux processes, A Century of Weather Progress. Pp. 35-44, Am. Met. Soc.

____

1971 Lecture to seminar on Civil Engineering, The University of Delaware, Spring 1971.

PHILLIPS, O.M.

1966 *The Dynamics of the Upper Ocean.* Cambridge University Press, 1966, 261 pp.

PRIESTLEY, C.H.B.

1959 *Turbulent Transfer in the Lower Atmosphere.* University of Chicago Press, 130 pp.

RUGGLES, KENNETH W.

1970 The vertical mean wind profile over the ocean for light to moderate winds. J. Appl. Met. *9*(3), 389-395, June 1970.

SHEMDIN

1969 Instantaneous velocity and pressure measurements above propagating waves. Tech. Rept. 4, Department of Coastal and Oceanographic Engineering, University of Florida.

__________ and E.Y. HSU

1966 The dynamics of wind in the vicinity of progressive water waves. Stanford University, Department of Civil Engineering, Report No. 66 (AD488-373).

TAKEDA, A.

1963 Wind profiles over sea waves. J. Ocean. Soc. Japan *19*, 16-22.

THORNTHWAITE, C.W., W.J. SUPERIOR, F.K. HARE, and K.R. ONO

1959 Measurement of vertical winds in typical terrain. Publications in Climatology *XII*(3).

__________, W.J. SUPERIOR, and J.R. MATHER

1961 Vertical winds near the ground at Centerton, N.J. Publications in Climatology *XIV*(2).

APPENDIX

Data Compiled from the Runs Used in the Study, by Run

Run: 1 Date: 20 Mar 71 Tape: 2 Section: 1

Run Length: 16.5 min

Temperatures: 4.5 C at 1.5 m and 4.85 C at 0.5 m

Number of Flags: 1 Intermittency: 0.61

Six Level Combined Data

z m	4	2	1	0.5	0.25	0.125
U m/s	8.76	7.98	7.22	6.39	5.93	4.92

u^*: 0.434 m/s z_o: 0.00126 m Corr. coeff.: 0.997 U_{10}: 9.739 m/s

Three Level Combined Data

z m	0.5	0.25	0.125	z_o: 0.00141 m u^*: 0.444 m/s
U m/s	6.39	5.93	4.92	Corr. coeff.: 0.977

U_{10}: 9.841 m/s u^{*2}/E_{20}: 0.0011

Three Level With Bursts Only

z m	0.5	0.25	0.125	z_o: 0.00176 m u^*: 0.522 m/s
U m/s	7.26	6.63	5.50	Corr. coeff.: 0.987

U_{10}: 11.271 m/s u^{*2}/E_{20}: 0.0011

Three Level With Bursts Omitted

z m	0.5	0.25	0.125	z_o: 0.00202 m u^*: 0.394 m/s
U m/s	5.38	4.83	4.03	Corr. coeff.: 0.994

U_{10}: 8.382 m/s u^{*2}/E_{20}: 0.0029

Run: 2 Date: 20 Mar 71 Tape: 2 Section: 2

Run Length: 16.5 min

Temperatures: 3.85 C at 1.5 m and 3.9 C at 0.5 m

Number of Flags: none Intermittency: 0.70

Six Level Combined Data

z m	4	2	1	0.5	0.25	0.125
U m/s	7.54	6.84	6.22	5.49	4.91	4.23

u*: 0.381 m/s z_o: 0.00148 m Corr. coeff.: 1.000 U_{10}: 8.39 m/s

Three Level Combined Data

z m	0.5	0.25	0.125	z_o: 0.00118 m u*: 0.364 m/s
U m/s	5.49	4.91	4.23	Corr. coeff.: 1.000

U_{10}: 8.238 m/s u^{*2}/E_{20}: 0.0014

Three Level With Bursts Only

z m	0.5	0.25	0.125	z_o: 0.00164 m u*: 0.425 m/s
U m/s	6.06	5.38	4.59	Corr. coeff: 0.999

U_{10}: 9.262 m/s u^{*2}/E_{20}: 0.0015

Three Level With Bursts Omitted

z m	0.5	0.25	0.125	z_o: 0.00237 m u*: 0.336 m/s
U m/s	4.53	3.84	3.38	Corr. coeff.: 0.993

U_{10}: 7.015 m/s u^{*2}/E_{20}: 0.0036

Run: 3 Date: 25 Mar 71 Tape: 1 Section: 1

Run Length: 10.5 min

Temperatures: 0.75 C at 1.5 m and 1.25 C at 0.5 m

Number of Flags: none Intermittency: 0.63

Six Level Combined Data

z m	4	2	1	0.5	0.25	0.125
U m/s	5.53	4.96	4.47	4.01	3.64	2.92

u*: 0.290 m/s z_o: 0.00200 m Corr. coeff.: 0.997 U_{10}: 6.176 m/s

Three Level Combined Data

z m	0.5	0.25	0.125	z_o: 0.00328 m u*: 0.325 m/s
U m/s	4.01	3.64	2.92	Corr. coeff.: 0.983

U_{10}: 6.522 m/s u^{*2}/E_{20}: 0.0038

Three Level With Bursts Only

z m	0.5	0.25	0.125	z_o: 0.00520 m u*: 0.406 m/s
U m/s	4.60	3.98	3.20	Corr. coeff.: 0.998

U_{10}: 7.669 m/s u^{*2}/E_{20}: 0.0046

Three Level With Bursts Omitted

z m	0.5	0.25	0.125	z_o: 0.00405 m u*: 0.287 m/s
U m/s	3.40	3.05	2.43	Corr. coeff.: 0.987

U_{10}: 5.608 m/s u^{*2}/E_{20}: 0.0058

Run: 4 Date: 25 Mar 71 Tape: 1 Section: 2

Run Length: 10.75 min

Temperatures: 0.9 C at 1.5 m and 1.6 C at 0.5 m

Number of Flags: 1 Intermittency: 0.67

Six Level Combined Data

z m	4	2	1	0.5	0.25	0.125
U m/s	5.60	5.04	4.55	4.09	3.68	3.13

u^*: 0.279 m/s z_o: 0.00139 m Corr. coeff.: 0.999 U_{10}: 6.198 m/s

Three Level Combined Data

z m	0.5	0.25	0.125	z_o: 0.00137 m u^*: 0.279 m/s
U m/s	4.09	3.68	3.13	Corr. coeff.: 0.996

U_{10}: 6.203 m/s u^{*2}/E_{20}: 0.0016

Three Level With Bursts Only

z m	0.5	0.25	0.125	z_o: 0.00215 m u^*: 0.346 m/s
U m/s	4.72	4.11	3.52	Corr. coeff.: 1.000

U_{10}: 7.312 m/s u^{*2}/E_{20}: 0.0018

Three Level With Bursts Omitted

z m	0.5	0.25	0.125	z_o: 0.00148 m u^*: 0.214 m/s
U m/s	3.08	2.79	2.35	Corr. coeff.: 0.993

U_{10}: 4.708 m/s u^{*2}/E_{20}: 0.0046

Run: 5 Date: 25 Mar 71 Tape: 1 Section: 3

Run Length: 10.25 min

Temperatures: 1.5 C at 1.5 m and 2.00 C at 0.5 m

Number of Flags: 1 Intermittency: 0.60

Six Level Combined Data

z m	4	2	1	0.5	0.25	0.125
U m/s	5.18	4.65	4.16	3.70	3.40	2.88

$u*$: 0.260 m/s z_o: 0.00153 m Corr. coeff.: 0.997 U_{10}: 5.719 m/s

Three Level Combined Data

z m	0.5	0.25	0.125
U m/s	3.70	3.40	2.88

z_o: 0.00103 m $u*$: 0.242 m/s

Corr. coeff.: 0.988

U_{10}: 5.561 m/s

$u*^2/E_{20}$: 0.0033

Three Level With Bursts Only

z m	0.5	0.25	0.125
U m/s	4.15	3.84	3.26

z_o: 0.000864 m $u*$: 0.265 m/s

Corr. coeff.: 0.985

U_{10}: 6.192 m/s

$u*^2/E_{20}$: 0.0028

Three Level With Bursts Omitted

z m	0.5	0.25	0.125
U m/s	2.86	2.75	2.30

z_o: 0.000747 m $u*$: 0.181 m/s

Corr. coeff.: 0.944

U_{10}: 4.309 m/s

$u*^2/E_{20}$: 0.0044

Run: 6 Date: 8 April 71 Tape: 1 Section: 1

Run Length: 10.0 min

Temperatures: 7.8 C at 1.0 m and 8.5 C at 0.2 m

Number of Flags: 5 Intermittency: 0.82

Six Level Combined Data

z m	4	2	1	0.25	0.12	0.06
U m/s	7.66	6.81	6.07	4.78	4.48	3.55

u*: 0.377 m/s z_o: 0.00135 m Corr. coeff.: 0.995 U_{10}: 8.390 m/s

Three Level Combined Data

z m	0.25	0.12	0.06	z_o: 0.00131 m u*: 0.377 m/s
U m/s	4.78	4.48	3.55	Corr. coeff.: 0.954

U_{10}: 8.418 m/s u^{*2}/E_{20}: 0.00041

Three Level With Bursts Only

z m	0.25	0.12	0.06	z_o: 0.000993 m u*: 0.371 m/s
U m/s	4.94	4.68	3.75	Corr. coeff.: 0.946

U_{10}: 8.543 m/s u^{*2}/E_{20}: 0.00033

Three Level With Bursts Omitted

z m	0.25	0.12	0.06	z_o: 0.00245 m u*: 0.330 m/s
U m/s	3.48	3.53	2.66	Corr. coeff.: 0.83

U_{10}: 6.854 m/s u^{*2}/E_{20}: 0.0019

Run: 7 Date: 8 April 71 Tape: 1 Section: 2

Run Length: 11.0 min

Temperatures: 7.9 C at 1.0 m and 8.6 C at 0.2 m

Number of Flags: 4 Intermittency: 0.39

Six Level Combined Data

z m	4	2	1	0.25	0.12	0.06
U m/s	7.07	6.35	5.68	4.50	4.15	3.28

u^*: 0.348 m/s z_o: 0.00129 m Corr. coeff.: 0.997 U_{10}: 7.788 m/s

Three Level Combined Data

z m	0.25	0.12	0.06
U m/s	4.50	4.15	3.28

z_o: 0.00154 m u^*: 0.364 m/s

Corr. coeff.: 0.967

U_{10}: 7.995 m/s u^{*2}/E_{20}: 0.00060

Three Level With Bursts Only

z m	0.25	0.12	0.06
U m/s	5.21	4.91	3.84

z_o: 0.00155 m u^*: 0.427 m/s

Corr. coeff.: 0.946

U_{10}: 9.362 m/s u^{*2}/E_{20}: 0.00044

Three Level With Bursts Omitted

z m	0.25	0.12	0.06
U m/s	4.02	3.66	2.93

z_o: 0.00143 m u^*: 0.318 m/s

Corr. coeff.: 0.978

U_{10}: 7.043 m/s u^{*2}/E_{20}: 0.00099

Run: 8 Date: 8 April 71 Tape: 1 Section: 3

Run Length: 11.0 min

Temperatures: 8.1 C at 1.0 m and 8.85 C at 0.2 m

Number of Flags: 4 Intermittency: 0.56

Six Level Combined Data

z m	4	2	1	0.25	0.12	0.06
U m/s	8.79	7.81	6.94	5.69	5.52	4.36

u^*: 0.399 m/s z_o: 0.000716 m Corr. coeff.: 0.988 U_{10}: 9.521 m/s

Three Level Combined Data

z m	0.25	0.12	0.06	z_o: 0.00114 m u^*: 0.445 m/s
U m/s	5.69	5.52	4.36	Corr. coeff.: 0.912

U_{10}: 10.099 m/s u^{*2}/E_{20}: 0.00022

Three Level With Bursts Only

z m	0.25	0.12	0.06	z_o: 0.00112 m u^*: 0.491 m/s
U m/s	6.40	6.05	4.82	Corr. coeff.: 0.947

U_{10}: 11.176 m/s u^{*2}/E_{20}: 0.00019

Three Level With Bursts Omitted

z m	0.25	0.12	0.06	z_o: 0.00149 m u^*: 0.414 m/s
U m/s	5.08	4.82	3.77	Corr. coeff.: 0.939

U_{10}: 9.121 m/s u^{*2}/E_{20}: 0.00040

Run: 9 Date: 8 April 71 Tape: 2 Section: 1

Run Length: 10.5 min

Temperatures: 9.2 C at 1.0 m and 9.85 C at 0.2 m

Number of Flags: 3 Intermittency: 0.59

Six Level Combined Data

z m	4	2	1	0.25	0.06	0.03
U m/s	8.05	7.25	6.50	5.14	4.49	4.10

u_*: 0.328 m/s z_o: 0.000287 m Corr. coeff.: 0.986 U_{10}: 8.58 m/s

Three Level Combined Data

z m	0.25	0.06	0.03	z_o: 0.0000063 m u_*: 0.195 m/s
U m/s	5.14	4.49	4.10	Corr. coeff.: 0.998

U_{10}: 6.948 m/s u_*^2/E_{20}: 0.00007

Three Level With Bursts Only

z m	0.25	0.06	0.03	z_o: 0.0000025 m u_*: 0.198 m/s
U m/s	5.69	4.99	4.64	Corr. coeff.: 1.000

U_{10}: 7.518 m/s u_*^2/E_{20}: 0.000048

Three Level With Bursts Omitted

z m	0.25	0.06	0.03	z_o: 0.0000014 m u_*: 0.136 m/s
U m/s	4.07	3.71	3.35	Corr. coeff.: 0.981

U_{10}: 5.359 m/s u_*^2/E_{20}: 0.00010

Run: 10 Date: 8 April 71 Tape: 2 Section: 2

Run Length: 11.0 min

Temperatures: 10.2 C at 1.0 m and 10.8 C at 0.2 m

Number of Flags: 4 Intermittency: 0.50

Six Level Combined Data

z m	4	2	1	0.25	0.06	0.03
U m/s	6.74	6.04	5.39	4.27	3.49	3.24

u*: 0.292 m/s z_o: 0.000499 m Corr. coeff.: 0.991 U_{10}: 7.225 m/s

Three Level Combined Data

z m	0.25	0.06	0.03	z_o: 0.000494 m u*: 0.200 m/s
U m/s	4.27	3.49	3.24	Corr. coeff.: 0.996

U_{10}: 4.948 m/s u^{*2}/E_{20}: 0.00020

Three Level With Bursts Only

z m	0.25	0.06	0.03	z_o: 0.000723 m u*: 0.238 m/s
U m/s	4.85	3.97	3.60	Corr. coeff.: 0.999

U_{10}: 5.665 m/s u^{*2}/E_{20}: 0.00018

Three Level With Bursts Omitted

z m	0.25	0.06	0.03	z_o: 0.000126 m u*: 0.203 m/s
U m/s	3.87	3.02	2.87	Corr. coeff.: 0.983

U_{10}: 5.727 m/s u^{*2}/E_{20}: 0.00044

Run: 11 Date: 8 April 71 Tape: 2 Section: 3

Run Length: 10.5 min

Temperatures: 10.5 C at 1.0 m and 11 C at 0.2 m

Number of Flags: 3 Intermittency: 0.77

Six Level Combined Data

z m	4	2	1	0.25	0.06	0.03
U m/s	7.88	7.04	6.31	4.92	4.07	3.81

u^*: 0.342 m/s z_o: 0.000515 m Corr. coeff.: 0.988 U_{10}: 8.439 m/s

Three Level Combined Data

z m	0.25	0.06	0.03	z_o: 0.0000283 m	u^*: 0.216 m/s
U m/s	4.92	4.07	3.81	Corr. coeff.: 0.995	
U_{10}: 6.894 m/s				u^{*2}/E_{20}: 0.0010	

Three Level With Bursts Only

z m	0.25	0.06	0.03	z_o: 0.0000487 m	u^*: 0.247 m/s
U m/s	5.30	4.31	4.04	Corr. coeff.: 0.993	
U_{10}: 7.560 m/s				u^{*2}/E_{20}: 0.00011	

Three Level With Bursts Omitted

z m	0.25	0.06	0.03	z_o: 0.0000559 m	u^*: 0.190 m/s
U m/s	4.00	3.26	3.02	Corr. coeff.: 0.996	
U_{10}: 5.737 m/s				u^{*2}/E_{20}: 0.00025	

Run: 12 Date: 8 April 71 Tape: 3 Section: 1

Run Length: 10.25 min

Temperatures: 10.4 C at 1.0 m and 11.0 C at 0.2 m

Number of Flags: 2 Intermittency: 0.27

Six Level Combined Data

z m	4	2	1	0.25	0.06	0.03
U m/s	7.81	7.04	6.30	5.02	3.95	3.23

u^*: 0.367 m/s z_o: 0.000909 m Corr. coeff.: 0.998 U_{10}: 8.530 m/s

Three Level Combined Data

z m	0.25	0.06	0.03
U m/s	5.02	3.95	3.23

z_o: 0.000592 m u^*: 0.334 m/s

Corr. coeff.: 0.996

U_{10}: 8.139 m/s

u^{*2}/E_{20}: 0.00032

Three Level With Bursts Only

z m	0.25	0.06	0.03
U m/s	5.94	4.96	3.91

z_o: 0.000452 m u^*: 0.385 m/s

Corr. coeff.: 0.977

U_{10}: 9.620 m/s

u^{*2}/E_{20}: 0.00018

Three Level With Bursts Omitted

z m	0.25	0.06	0.03
U m/s	4.69	3.55	2.98

z_o: 0.000737 m u^*: 0.322 m/s

Corr. coeff.: 1.000

U_{10}: 7.661 m/s

u^{*2}/E_{20}: 0.00075

Run: 13 Date: 8 April 71 Tape: 3 Section: 2

Run Length: 10.5 min

Temperatures: 11.0 C at 1.0 m and 11.5 C at 0.2 m

Number of Flags: 1 Intermittency: 0.54

Six Level Combined Data

z m	4	2	1	0.25	0.06	0.03
U m/s	7.02	6.28	5.58	4.45	3.24	2.61

u^*: 0.354 m/s z_o: 0.00161 m Corr. coeff.: 0.999 U_{10}: 7.729 m/s

Three Level Combined Data

z m	0.25	0.06	0.03	z_o: 0.00145 m u^*: 0.346 m/s
U m/s	4.45	3.24	2.61	Corr. coeff.: 0.999

U_{10}: 7.646 m/s u^{*2}/E_{20}: 0.00078

Three Level With Bursts Only

z m	0.25	0.06	0.03	z_o: 0.00130 m u^*: 0.379 m/s
U m/s	4.97	3.67	2.95	Corr. coeff.: 0.999

U_{10}: 8.481 m/s u^{*2}/E_{20}: 0.00061

Three Level With Bursts Omitted

z m	0.25	0.06	0.03	z_o: 0.00108 m u^*: 0.268 m/s
U m/s	3.64	2.72	2.21	Corr. coeff.: 0.999

U_{10}: 6.126 m/s u^{*2}/E_{20}: 0.0013

Run: 14 Date: 8 April 71 Tape: 3 Section: 3

Run Length: 10.5 min

Temperatures: 10.8 C at 1.0 m and 11.4 C at 0.2 m

Number of Flags: 3 Intermittency: 0.48

Six Lev… …mbined Date

z m	4	2	1	0.25	0.06	0.03
U m/s	6.76	6.05	5.44	4.35	3.62	2.80

u^*: 0.309 m/s z_o: 0.000751 m Corr. coeff.: 0.995 U_{10}: 7.339 m/s

Three Level Combined Data

z m	0.25	0.06	0.03	z_o: 0.000587 m u^*: 0.295 m/s
U m/s	4.35	3.62	2.80	Corr. coeff.: 0.973

U_{10}: 7.180 m/s u^{*2}/E_{20}: 0.00050

Three Level With Bursts Only

z m	0.25	0.06	0.03	z_o: 0.000479 m u^*: 0.342 m/s
U m/s	5.11	4.49	3.40	Corr. coeff.: 0.938

U_{10}: 8.494 m/s u^{*2}/E_{20}: 0.00039

Three Level With Bursts Omitted

z m	0.25	0.06	0.03	z_o: 0.000815 m u^*: 0.254 m/s
U m/s	3.60	2.82	2.24	Corr. coeff.: 0.994

U_{10}: 5.982 m/s u^{*2}/E_{20}: 0.0013

Run: 15 Date: 8 April 71 Tape: 4 Section: 1

Run Length: 11.5 min

Temperatures: 10.75 C at 1.0 m and 11.3 C at 0.2 m

Number of Flags: 4 Intermittency: 0.29

Six Level Combined Data

z m	4	2	1	0.25	0.06	0.03
U m/s	5.75	5.22	4.76	3.83	3.36	2.52

u^*: 0.250 m/s z_o: 0.000446 m Corr. coeff.: 0.992 U_{10}: 6.265 m/s

Three Level Combined Data

z m	0.25	0.06	0.03	z_o: 0.000550 m u^*: 0.262 m/s
U m/s	3.83	3.36	2.52	Corr. coeff.: 0.936

U_{10}: 6.432 m/s u^{*2}/E_{20}: 0.00066

Three Level With Bursts Only

z m	0.25	0.06	0.03	z_o: 0.000304 m u^*: 0.313 m/s
U m/s	5.09	4.43	3.48	Corr. coeff.: 0.955

U_{10}: 8.151 m/s u^{*2}/E_{20}: 0.00030

Three Level With Bursts Omitted

z m	0.25	0.06	0.03	z_o: 0.000702 m u^*: 0.235 m/s
U m/s	3.25	2.91	2.12	Corr. coeff.: 0.912

U_{10}: 5.626 m/s u^{*2}/E_{20}: 0.0019

Run: 16 Date: 8 April 71 Tape: 4 Section: 2

Run Length: 11.0 min

Temperatures: 11.15 C at 1.0 m and 11.72 C at 0.2 m

Number of Flags: 5 Intermittency: 0.58

Six Level Combined Data

z m	4	2	1	0.25	0.06	0.03
U m/s	7.22	6.47	5.81	4.60	4.03	3.12

u^*: 0.32 m/s z_o: 0.000584 m Corr. coeff.: 0.991 U_{10}: 7.799 m/s

Three Level Combined Data

z m	0.25	0.06	0.03	z_o: 0.000357 m u^*: 0.231 m/s
U m/s	4.60	4.03	3.12	Corr. coeff.: 0.946

U_{10}: 7.469 m/s u^{*2}/E_{20}: 0.00019

Three Level With Bursts Only

z m	0.25	0.06	0.03	z_o: 0.000359 m u^*: 0.346 m/s
U m/s	5.52	4.70	3.71	Corr. coeff.: 0.969

U_{10}: 8.361 m/s u^{*2}/E_{20}: 0.00027

Three Level With Bursts Omitted

z m	0.25	0.06	0.03	z_o: 0.000534 m u^*: 0.238 m/s
U m/s	3.47	3.10	2.31	Corr. coeff.: 0.920

U_{10}: 5.863 m/s u^{*2}/E_{20}: 0.00090

Run: 17 Date: 8 April 71 Tape: 4 Section: 3

Run Length: 10.5 min

Temperatures: 11.3 C at 1.0 m and 11.65 C at 0.2 m

Number of Flags: 2 Intermittency: 0.63

Six Level Combined Data

z m	4	2	1	0.25	0.06	0.03
U m/s	7.31	6.68	6.09	4.84	4.22	3.24

u^*: 0.319 m/s z_o: 0.000456 m Corr. coeff.: 0.993 U_{10}: 7.984 m/s

Three Level Combined Data

z m	0.25	0.06	0.03	z_o: 0.000421 m u^*: 0.315 m/s
U m/s	4.84	4.22	3.24	Corr. coeff.: 0.947

U_{10}: 7.933 m/s u^{*2}/E_{20}: 0.00032

Three Level With Bursts Only

z m	0.25	0.06	0.03	z_o: 0.000506 m u^*: 0.352 m/s
U m/s	5.17	4.63	3.46	Corr. coeff.: 0.918

U_{10}: 8.707 m/s u^{*2}/E_{20}: 0.00029

Three Level With Bursts Omitted

z m	0.25	0.06	0.03	z_o: 0.000189 m u^*: 0.232 m/s
U m/s	4.10	3.49	2.87	Corr. coeff.: 0.980

U_{10}: 6.316 m/s u^{*2}/E_{20}: 0.00050

Run: 18 Date: 10 April 71 Tape: 1 Section: 1

Run Length: 5.5 min

Temperatures: 8.8 C at 1.0 m and 9.3 C at 0.2 m

Number of Flags: 2 Intermittency: 0.76

Six Level Combined Data

z m	4	2	1	0.25	0.125	0.058
U m/s	9.30	8.40	7.64	5.94	4.95	4.40

u^*: 0.476 m/s z_o: 0.00167 m Corr. coeff.: 0.998 U_{10}: 10.354 m/s

Three Level Combined Data

z m	0.25	0.125	0.058
U m/s	5.94	4.95	4.40

z_o: 0.00113 m u^*: 0.435 m/s

Corr. coeff.: 0.981

U_{10}: 9.889 m/s u^{*2}/E_{20}: 0.00056

Three Level With Bursts Only

z m	0.25	0.125	0.058
U m/s	6.22	5.25	4.67

z_o: 0.000868 m u^*: 0.435 m/s

Corr. coeff.: 0.985

U_{10}: 10.176 m/s u^{*2}/E_{20}: 0.00046

Three Level With Bursts Omitted

z m	0.25	0.125	0.058
U m/s	4.83	3.99	3.56

z_o: 0.00127 m u^*: 0.362 m/s

Corr. coeff.: 0.977

U_{10}: 8.112 m/s u^{*2}/E_{20}: 0.0010

Run: 19 Date: 10 April 71 Tape: 1 Section: 2

Run Length: 5.0 min

Temperatures: 8.5 C at 1.0 m and 9.0 C at 0.2 m

Number of Flags: 7 Intermittency: 0.65

Six Level Combined Data

z m	4	2	1	0.25	0.125	0.058
U m/s	9.19	8.39	7.58	5.45	4.64	4.32

u^*: 0.501 m/s z_o: 0.00254 m Corr. coeff.: 0.993 U_{10}: 10.361 m/s

Three Level Combined Data

z m	0.25	0.125	0.058
U m/s	5.45	4.64	4.32

z_o: 0.000369 m u^*: 0.331 m/s

Corr. coeff.: 0.962

U_{10}: 8.450 m/s u^{*2}/E_{20}: 0.00026

Three Level With Bursts Only

z m	0.25	0.125	0.058
U m/s	6.02	5.15	4.88

z_o: 0.000242 m u^*: 0.344 m/s

Corr. coeff.: 0.948

U_{10}: 9.139 m/s u^{*2}/E_{20}: 0.00020

Three Level With Bursts Omitted

z m	0.25	0.125	0.058
U m/s	4.55	3.70	3.29

z_o: 0.00172 m u^*: 0.361 m/s

Corr. coeff.: 0.974

U_{10}: 7.823 m/s u^{*2}/E_{20}: 0.0010

Run: 20 Date: 10 April 71 Tape: 1 Section: 3

Run Length: 8.0 min

Temperatures: 8.65 C at 1.0 m and 9.25 C at 0.2 m

Number of Flags: 6 Intermittency: 0.58

Six Level Combined Data

z m	4	2	1	0.25	0.125	0.058
U m/s	9.56	8.64	7.72	6.02	5.11	4.80

u^*: 0.474 m/s z_o: 0.00138 m Corr. coeff.: 0.994 U_{10}: 10.544 m/s

Three Level Combined Data

z m	0.25	0.125	0.058
U m/s	6.02	5.11	4.80

z_o: 0.000356 m u^*: 0.364 m/s

Corr. coeff.: 0.953

U_{10}: 9.320 m/s

u^{*2}/E_{20}: 0.00032

Three Level With Bursts Only

z m	0.25	0.125	0.058
U m/s	6.59	5.54	5.27

z_o: 0.00041 m u^*: 0.408 m/s

Corr. coeff.: 0.936

U_{10}: 10.298 m/s

u^{*2}/E_{20}: 0.00030

Three Level With Bursts Omitted

z m	0.25	0.125	0.058
U m/s	5.22	4.51	4.14

z_o: 0.000296 m u^*: 0.307 m/s

Corr. coeff.: 0.978

U_{10}: 8.003 m/s

u^{*2}/E_{20}: 0.00047

Run: 21 Date: 10 April 71 Tape: 1 Section: 4

Run Length: 6.0 min

Temperatures: 8.8 C at 1.0 m and 9.5 C at 0.2 m

Number of Flags: 5 Intermittency: 0.63

Six Level Combined Data

z m	4	2	1	0.25	0.125	0.058
U m/s	9.01	8.18	7.27	5.49	4.70	4.30

u^*: 0.470 m/s z_o: 0.00197 m Corr. coeff.: 0.995 U_{10}: 10.026 m/s

Three Level Combined Data

z m	0.25	0.125	0.058
U m/s	5.49	4.70	4.30

z_o: 0.00041 m u^*: 0.339 m/s

Corr. coeff.: 0.976

U_{10}: 8.568 m/s u^{*2}/E_{20}: 0.00039

Three Level With Bursts Only

z m	0.25	0.125	0.058
U m/s	5.93	5.20	4.70

z_o: 0.000254 m u^*: 0.342 m/s

Corr. coeff.: 0.991

U_{10}: 9.043 m/s u^{*2}/E_{20}: 0.00029

Three Level With Bursts Omitted

z m	0.25	0.125	0.058
U m/s	4.69	3.91	3.61

z_o: 0.000724 m u^*: 0.317 m/s

Corr. coeff.: 0.961

U_{10}: 7.566 m/s u^{*2}/E_{20}: 0.00083

Run: 22 Date: 10 April 71 Tape: 1 Section: 5

Run Length: 7.0 min

Temperatures: 8.9 C at 1.0 m and 9.8 C at 0.2 m

Number of Flags: 4 Intermittency: 0.65

Six Level Combined Data

z m	4	2	1	0.25	0.125	0.058
U m/s	7.34	6.61	5.97	4.69	3.80	3.43

u^*: 0.381 m/s z_o: 0.00189 m Corr. coeff.: 0.997 U_{10}: 8.173 m/s

Three Level Combined Data

z m	0.25	0.125	0.058	z_o: 0.00161 m u^*: 0.367 m/s
U m/s	4.69	3.80	3.43	Corr. coeff.: 0.966

U_{10}: 8.013 m/s u^{*2}/E_{20}: 0.00094

Three Level With Bursts Only

z m	0.25	0.125	0.058	z_o: 0.00118 m u^*: 0.379 m/s
U m/s	5.13	4.16	3.89	Corr. coeff.: 0.941

U_{10}: 8.573 m/s u^{*2}/E_{20}: 0.00072

Three Level With Bursts Omitted

z m	0.25	0.125	0.058	z_o: 0.00410 m u^*: 0.377 m/s
U m/s	3.91	3.15	2.54	Corr. coeff.: 0.996

U_{10}: 7.358 m/s u^{*2}/E_{20}: 0.0031